Comprehensive analysis of type 1 fimbriae regulation in *fimB*-null strains from the multidrug resistant *Escherichia coli* ST131 clone

Sohinee Sarkar[1,2,3], Leah W. Roberts[1,2], Minh-Duy Phan[1,2], Lendl Tan[1,2], Alvin W. Lo[1,2], Kate M. Peters[1,2], David L. Paterson[2,4], Mathew Upton[5], Glen C. Ulett[6], Scott A. Beatson[1,2*], Makrina Totsika[1,2,3*] and Mark A. Schembri[1,2*]

[1]School of Chemistry and Molecular Biosciences, The University of Queensland, Brisbane, Queensland, 4072, Australia

[2]Australian Infectious Disease Research Centre, The University of Queensland, Brisbane, Queensland, 4072, Australia

[3]Institute of Health and Biomedical Innovation, School of Biomedical Sciences, Queensland

[4]University of Technology, Brisbane, Queensland, 4059, Australia

[5]University of Queensland Centre for Clinical Research, Royal Brisbane and Women's Hospital, Brisbane, Queensland, 4029, Australia

[6]Plymouth University Peninsula Schools of Medicine and Dentistry, Plymouth, PL6 8BU, United Kingdom

[7]School of Medical Science, Menzies Health Institute Queensland, Griffith University, Gold Coast, Queensland, 4222, Australia

Running title: Regulation of type 1 fimbriae in *E. coli* ST131

Keywords: uropathogenic *E. coli*, type 1 fimbriae, ST131, regulation, urinary tract infection

* For correspondence. E-mail m.schembri@uq.edu.au, makrina.totsika@qut.edu.au or s.beatson@uq.edu.au; Tel: 61 7 33653306.

Summary

Uropathogenic *Escherichia coli* (UPEC) of sequence type 131 (*E. coli* ST131) are a pandemic multidrug resistant clone associated with urinary tract and bloodstream infections. Type 1 fimbriae, a major UPEC virulence factor, are essential for ST131 bladder colonization. The globally dominant sub-lineage of ST131 strains, clade C/*H*30-R, possess an IS*Ec55* insertion in the *fimB* gene that controls phase-variable type 1 fimbriae expression via the invertible *fimS* promoter. We report that the inactivation of *fimB* in these strains causes altered regulation of type 1 fimbriae expression. Using a novel molecular approach, we demonstrate that 'off' to 'on' *fimS* inversion is reduced in these strains and mediated by the *fimE* and *fimX* genes. Unlike typical UPEC strains, the nucleoid-associated H-NS protein does not strongly repress *fimE* transcription in these strains. Using a genetic screen to identify novel regulators of *fimE* and *fimX* in the clade C/*H*30-R ST131 strain EC958, we defined a new role for the *guaB* gene as a regulator of type 1 fimbriae and a mouse bladder colonization factor. Our results provide a comprehensive analysis of type 1 fimbriae regulation in the globally predominant group of ST131 strains, and highlight important differences in its control compared to non-ST131 UPEC.

Introduction

Uropathogenic *Escherichia coli* (UPEC) are the leading cause of urinary tract infection (UTI), resulting in over 150 million cases worldwide every year (1) and amounting to billions of dollars spent in direct and associated healthcare costs (2). The increased incidence of UTIs caused by multidrug resistant (MDR) strains, including strains that belong to high-risk globally pandemic clones such as *E. coli* sequence type 131 (*E. coli* ST131), presents significant new challenges for the management and treatment of UTI.

E. coli ST131 is a globally disseminated MDR clone originally identified due to its close association with the spread of the $bla_{\text{CTX-M-15}}$ extended spectrum β-lactamase (ESBL) gene (3-5). Genomic analysis of *E. coli* ST131 has identified a globally dominant fluoroquinolone resistant-*fimH*30 subgroup previously defined as *H*30-R (6) or clade C (7), as well as two additional less prevalent clades (referred to as A and B) (7). Type 1 fimbriae represent the best-characterized *E. coli* ST131 virulence factor and are required for ST131 colonization of the mouse bladder (8). Its pharmacological inhibition has been shown to prevent the establishment of acute MDR UTI and treat chronic bladder infection in mice (9).

The *E. coli* type 1 fimbriae (*fim*) gene cluster contains nine genes, which encode the major (FimA) and minor (FimFGH) structural components, the chaperone-usher transport and assembly apparatus (FimCD) and two regulatory proteins (FimB and FimE) (10, 11). Type 1 fimbrial expression is phase variable due to inversion of the *fim* switch (*fimS*), a 314 bp invertible DNA element which contains a promoter that drives transcription of the *fimACDFGH* genes (12). 'On' or 'off' orientation of *fimS* results in a fimbriated or bald phenotype, respectively. Two tyrosine-like

recombinases, FimB and FimE, catalyze the inversion of *fimS* (13). The FimB recombinase possesses bidirectional switching activity ('off'-to-'on' and 'on'-to-'off'), while FimE primarily catalyzes 'on'-to-'off' *fimS* inversion (13, 14). FimE can also mediate 'off'-to-'on' inversion of *fimS* under some growth conditions, but at lower efficiency (15, 16). The transcription of the *fimB* and *fimE* genes is driven by individual promoters, both of which are repressed by the histone-like nucleoid associated protein H-NS in *E. coli* K-12 strains (17). The inversion of *fimS* is subject to a complex regulatory network that involves several other global regulators, including integration host factor (IHF) (18) and the leucine-responsive regulatory protein (Lrp) (19), as well as other proteins that directly or indirectly impact on *fimS* orientation (reviewed in (20)). The 'off'-to-'on' switching of *fimS* is enhanced by growth in static liquid culture, which results in the enrichment of type 1 fimbriated cells and the formation of a pellicle at the air-liquid interface (21-23).

In addition to *fimB* and *fimE*, three other genes encoding tyrosine-like recombinases have been identified in UPEC (24). The products of two of these genes, FimX (24-26) and IpuA (24) can mediate *fimS* inversion. It has been shown that FimX possesses specificity for *fimS* 'off' to 'on' inversion, while IpuA can mediate bidirectional inversion (24, 26). In the reference UPEC strain UTI89, FimX mediates slow 'off' to 'on' *fimS* inversion *in vitro*, but rapid *fimS* 'on' switching during infection of the mouse bladder (25). The *fimX* gene is located adjacent to the *hyxR* gene at a site distal to the *fim* genes on the chromosome (25, 27). An invertible DNA switch analogous to *fimS* lies between the *fimX-hyxR* genes (27). FimX-mediated inversion of this *in cis* cognate switch influences the transcription of *hyxR*, which encodes a LuxR-like response regulator that controls tolerance to reactive nitrogen intermediates (27).

E. coli ST131 strains from the globally dominant clade C/*H*30-R group (hereafter referred to as clade C) possess a 1,895bp insertion element within the *fimB* recombinase gene (*fimB*::IS*Ec55*; Fig. 1) (8, 28). Given the role of *fimB* in *fimS* 'on' switching, it is therefore likely that the presence of this insertion affects type 1 fimbriae expression in ST131. Indeed, the *fimB*::IS*Ec55* insertion in ST131 has been associated with a slower 'off'-to-'on' switching phenotype *in vitro* (8).

In this study, we investigated the impact of the *fimB*::IS*Ec55* insertion on type 1 fimbriae expression by comparing ST131 strains that possessed either an intact or disrupted *fimB* gene. We confirmed that strains containing the *fimB*::IS*Ec55* insertion display slow 'off' to 'on' type 1 fimbriae switching phenotype and demonstrated its association with increased transcription of the *fimE* gene. Notably, H-NS repression of *fimE* in these strains was also altered compared to non-ST131 strains, highlighting an important difference in type 1 fimbriae regulation between ST131 strains and other well-characterized UPEC reference strains. We also examined the role of the FimE and FimX recombinases in *fimS* inversion in the ST131 clade C reference strain EC958, and described the use of a novel molecular approach based on Illumina deep sequencing to quantitate *fimS* orientation. Finally, we show that in EC958, guanosine 5' triphosphate (GTP) homeostasis and the bacterial stringent response triggered by the (p)ppGpp alarmone contribute to type 1 fimbriae expression via *fimE* and *fimX* regulation.

Results

Most E. coli ST131 strains can express type 1 fimbriae regardless of their fimB status

We previously sequenced a large collection of *E. coli* ST131 isolates from different geographical locations (7), including the high-quality reference genome of EC958, a representative clade C strain (8, 29). Despite most strains encoding intact and seemingly functional type 1 fimbriae operons, type 1 fimbriae expression was not a conserved trait among *E. coli* ST131 strains under standard laboratory growth (7, 8). This variability in type 1 fimbriae expression was significantly associated with the presence of an insertion element within the *fimB* recombinase gene that was identified in most clade C ST131 strains studied by us and others (7, 8, 28). Here, we extended these findings in a larger collection of 91 ST131 strains (71 previously published, detailed in Materials and Methods) for which we provide a comprehensive type 1 fimbriae expression profile. In this collection, 57 strains contained the *fimB*::IS*Ec55* insertion (and were from clade C) and 34 contained an intact *fimB* gene (and were from clades A and B). Using yeast cell agglutination, a standard method for monitoring the production of mannose-sensitive fimbriae (30), we determined type 1 fimbriae expression following growth in different conditions (Table 1). Following overnight shaking growth in LB broth at 37°C, only 14% of the *fimB*::IS*Ec55* containing strains expressed type 1 fimbriae compared to 70.6% of strains with an intact *fimB* gene, X^2 (1, N = 91) = 29.87, P<0.0001. This significant difference was also observed following overnight static growth, X^2 (1, N = 91) = 9.063, P<0.01, but no significant association was seen between *fimB* status and type 1 fimbriae expression when strains were further statically subcultured (Table 1; days 2 and 3). By three successive rounds of static subculture, the majority of ST131 strains were positive for type 1 fimbriae expression irrespective of *fimB* gene status. However, a step-wise increase in the proportion of type 1 positive strains was only seen for those

containing the *fimB::ISEc55* insertion, suggesting a slower rate of 'on' switching for most of these strains.

In our analysis, ten strains (five with an intact *fimB* and five with a *fimB::ISEc55* insertion) remained negative for type 1 fimbriae expression and were further subjected to six additional rounds of 24-hour static subculture. This resulted in the expression of type 1 fimbriae by four strains, three out of which had an intact *fimB* gene. Of the six remaining strains (S1, S18, S27, S36, S61, S77), S36 (Supporting Information Fig. S1) and S77 (7) had large deletions within coding regions of the type 1 fimbrial operon, accounting for their negative yeast agglutination phenotype. To test the capacity of *fimS* to invert to an 'on' orientation in S1, S18, S27 and S61, each strain was transformed with a plasmid containing the *fimB* gene from CFT073 (pFimB) and subjected to static culture followed by a screening PCR to determine *fimS* orientation (24). Over-expression of FimB in this manner resulted in *fimS* inversion to an 'on' orientation in three of the strains (S1, S18 and S61), however functional type 1 fimbriae expression as assessed by yeast cell agglutination could only be detected for S18 (Table 2). Sequence analysis of *fimS* from S27 revealed a single cytosine deletion (Supporting Information Fig. S2) 8bp downstream of the left inverted repeat in *fimS* (31), which may account for the 'locked off' status of *fimS* in this strain.

The transcription of fimE is enhanced in ST131 strains with a fimB::ISEc55 insertion

We hypothesized that the *fimB*::IS*Ec55* insertion may alter the transcription of the downstream *fimE* recombinase gene. In order to test this, we examined the level of *fimE* transcription using qRT-PCR in EC958 as well as four additional clade C ST131 strains with the same *fimB*::IS*Ec55* insertion (S4, S54, S60, S88), and compared this to the level of *fimE* transcription in four ST131

strains with an intact *fimB* gene (S17, S31, S55, S90). Strains were grown in M9 minimal glucose medium with aeration to mid-log phase for analysis. In all cases, the level of *fimE* transcription was significantly higher in strains with the *fimB*::IS*Ec55* insertion compared to strains with an intact *fimB* gene (overall 6.26-fold increase in *fimE*; Fig. 2A; $P<0.05$).

FimX is another accessory tyrosine recombinase that contributes to turning 'on' *fimS* in UPEC (32). Given that all nine ST131 strains used for this analysis also screened positive for the *fimX* gene by PCR, *fimX* transcript levels were also examined. There was no significant difference in *fimX* transcription between the two strain sets (Fig. 2B).

The fimB::ISEc55 insertion does not contain an additional fimE promoter

The transcription start site (TSS) of *fimE* has previously been mapped to a T residue 166 bases upstream of the GTG start codon in the *E. coli* K-12 strain VL751 (17). As we observed significantly higher *fimE* transcript levels in ST131 strains with the *fimB*::IS*Ec55* insertion, we hypothesized that there may be an additional promoter located within the insertion element that could drive *fimE* transcription. The *fimE* TSS was mapped using 5' RACE to a G residue 164 bases upstream of the start codon in all five of the *fimB*::IS*Ec55* ST131 strains tested (EC958, S4, S54, S60, S88; Fig. 3). As a control, we also mapped the TSS of *fimE* in one ST131 strain with an intact *fimB* gene (S90), and showed that it was identical. A consensus -35 (TTGTTA) and -10 (AAAATA) promoter sequence, separated by 18 bp, was conserved in all ST131 strains examined.

Since the TSS was conserved in all ST131 strains tested, consensus sequences of *fimE* promoter and coding regions (1074 bp) from clades A, B and C strains were constructed from previously published genome sequences (7) to ascertain if there were any differences that could explain the higher *fimE* transcription observed in clade C strains. These were compared to corresponding *fimE* sequences from two non-ST131 UPEC strains (CFT073 and UTI89) and *E. coli* K-12 strain MG1655 by multiple sequence alignment (Supporting Information Fig. S3). Sequences from ST131 clade A and C strains were 100% identical and closely related to *fimE* from MG1655. In contrast, the sequence of the *fimE* promoter and coding region from ST131 clade B strains contained several nucleotide changes, and was most similar to the corresponding sequence from CFT073 and UTI89. The most parsimonious explanation for our observation in light of the known phylogeny of ST131 (7) is an independent recombination in the *fimE* region of clade B strains after divergence from clade C. This is distinct from the previously reported *fimD-uxuR* recombination event in clade C that encompassed the *fimH*30 allele (28). Nucleotide changes in the coding region were synonymous with only a single amino acid substitution (V198A) found in FimE from clade B ST131 strains (also present in UTI89, Supporting Information Fig. S3). These changes, however, are unlikely to account for the increased *fimE* transcript levels observed in strains with the *fimB*::IS*Ec55* insertion, as this is exclusively found in clade C ST131 strains.

FimE and FimX are responsible for inverting fimS to the 'on' orientation in EC958

Despite the lack of an intact *fimB* gene, the majority of clade C ST131 strains still expressed functional type 1 fimbriae after multiple rounds of static growth, indicating that they possess an alternative recombinase capable of switching 'on' *fimS*. Based on genomic analysis, EC958 contains two tyrosine-like recombinase genes that have been shown to mediate inversion of *fimS*

in other *E. coli* strains; namely *fimE* (15) and *fimX* (24-26). We therefore constructed a series of isogenic mutants in EC958 lacking *fimE* (EC958*fimE*), *fimX* (EC958*fimX*) or both genes (EC958*fimE fimX*) and monitored their capacity to express type 1 fimbriae by yeast agglutination and western blot analysis (using an antibody against the major fimbrial subunit FimA) following static growth with repeated subculture over a period of 5 days (Fig. 4).

Type 1 fimbriae expression was detected in EC958 following 3 successive rounds of 24-hour static growth. In contrast, type 1 fimbriae expression by EC958*fimE* was delayed and only observed after 4 successive rounds of static growth, demonstrating a direct role for FimE in 'off' to 'on' *fimS* inversion (Fig. 4A). This also implicated a role for FimX in *fimS* inversion, and although the single EC958*fimX* mutant demonstrated a type 1 fimbriae expression profile identical to wild-type, the EC958*fimE fimX* double mutant failed to express type 1 fimbriae after prolonged static subculture for up to 5 days (Fig. 4A). This result was further validated by complementation of the EC958*fimE fimX* double mutant with a plasmid containing either *fimE* or *fimX* (pFimE or pFimX), both of which resulted in rapid type 1 fimbriae production within two days of static subculture (Fig. 4B). Thus, our data demonstrate that FimE is the major recombinase responsible for 'off' to 'on' *fimS* inversion in EC958, and that FimX can also mediate this switching mechanism, albeit less efficiently than FimE during *in vitro* static growth.

Direct quantitation of fim switching in EC958 using Illumina sequencing

In order to quantitate the efficiency of FimE- and FimX-mediated *fimS* inversion in EC958, we utilized a novel read-mapping method based on Illumina sequencing data that we refer to as DNA Invertible Switch Counter (or DISCus). EC958, EC958*fimE* and EC958*fimX* were grown

under static conditions as described in the previous section. Aliquots from the air-liquid interface of each subculture were harvested on days 1-5, and genomic DNA was extracted and sequenced using Illumina Technology. Using DISCus, we determined the percentage of reads that corresponded to either the 'on' or 'off' orientation of *fimS* at each time point by read mapping to *fimS* pseudo-reference sequences representing both orientations. The starting inoculum for these experiments was an overnight shaking culture, which possessed only 1% *fimS* 'on' reads. In the static subculture time course, EC958 produced a steadily increasing *fimS* 'on' switching profile, with a maximum of 71% 'on' reads at day 5 (Fig. 5A). EC958*fimX* produced a similar *fimS* switching profile, with the exception that 'on' switching was slower on day 2 compared to wild-type (Fig. 5A). In contrast, *fimS* 'on' switching in EC958*fimE* occurred at a significantly slower rate. Only 11.6% of 'on' reads were detected at day 4 of static subculture, which then increased to a level comparative to EC958 and EC958*fimX* at day 5. DISCus analysis of the EC958*fimE fimX* double mutant did not identify any significant *fimS* 'on' switching, supporting our observation that FimE and FimX are the only recombinases capable of inverting *fimS* in EC958. Overall, the quantitative *fimS* switching data closely paralleled the type 1 fimbriae expression analysis for each strain based on yeast agglutination and FimA protein production (Fig. 4).

To examine the specificity of FimE and FimX for *fimS* inversion in greater detail, we complemented the EC958*fimE fimX* double mutant by introduction of a plasmid containing *fimE* (pFimE) or *fimX* (pFimX). The EC958*fimE fimX* (pSU2718, empty vector control), EC958*fimE fimX*(pFimE) and EC958*fimE fimX*(pFimX) strains were subcultured by static growth over 3 days as described above, and DISCus was used to analyze the *fimS* orientation from Illumina sequences generated at each time point. Interestingly, data from these experiments demonstrated

that when the recombinases were over-expressed in this manner, FimX exhibited greater propensity for *fimS* 'off' to 'on' inversion than FimE (Fig. 5B).

FimE does not invert the fimX switch in EC958

The *fimX* switch, located between the *fimX-hyxR* genes, comprises two 16 bp inverted repeats flanking a 278 bp central region (27). In addition to mediating *in trans* inversion of *fimS* (27), FimX also mediates *in cis* bidirectional inversion of this switch. To assess this in greater detail, we analyzed the *fimX* switch inversion rate from the sequence data generated above. In the experiments that involved repeated static subculture of EC958, EC958*fimE* and EC958*fimX*, the *fimX* switch remained primarily in the 'off' orientation (92-97% 'off') throughout the 5-day static subculture period (Fig. 6A). However, in the experiments involving subculture of the complemented strains EC958*fimE fimX*(pFimE) and EC958*fimE fimX*(pFimX), and the control strain EC958*fimE fimX*(pSU2718), we observed very rapid FimX-mediated *fimX* switch inversion within a day (Fig. 6B). Taken together, these results demonstrate a rapid and strong interaction of FimX with its cognate switch. Furthermore, these results also demonstrate for the first time that FimE is unable to invert the *fimX* switch in EC958.

H-NS is not a major repressor of fimE gene expression in EC958

The histone-like nucleoid structuring protein (H-NS) is a global transcriptional regulator (33). H-NS has been shown to directly regulate type 1 fimbriae expression in *E. coli* K-12 by binding to sequences adjacent to and within *fimS* (34) and also to the promoters of *fimB* and *fimE* (17, 35). At 37°C, H-NS down-regulates *fimE* transcription and *hns* deletion leads to increased *fimE* promoter activity (35). We constructed a *hns* deletion in EC958 and three non-ST131 UPEC

strains (UTI89, 536 and IHE3034) and measured *fimE* transcript levels of all wild-type strains and corresponding *hns* mutants by qRT-PCR. At 37°C, deletion of *hns* led to significantly increased *fimE* transcription compared to the wild-type in all non-ST131 UPEC strains (Fig. 7B-D). However, in EC958, there was only a relatively small increase in *fimE* transcription in the *hns* mutant compared to the wild-type (Fig. 7A). Thus, H-NS does not strongly repress *fimE* transcription in EC958.

Identification of genes that affect fimE and fimX promoter activity in EC958

In order to investigate the regulation of the *fimE* and *fimX* genes in EC958, two promoter-reporter strains were generated. The *lacIZ* genes of EC958 were initially inactivated to generate strain EC958*lac*, and this strain was subsequently modified by inserting the *lacZ* gene as a chromosomally located transcriptional fusion to the *fimE* (EC958*fimE::lacZ*) or *fimX* (EC958*fimX::lacZ*) promoter. When grown on LB agar containing X-gal, EC958*fimE::lacZ* colonies were pale blue (indicating weak transcription) and EC958*fimX::lacZ* colonies were white (indicating no transcription). The two reporter strains were then subjected to Tn*5* mutagenesis; in each case 50,000-60,000 transposon mutants were generated and visually screened based on their blue colour intensity following growth on LB X-gal agar. Individual colonies that were dark blue (compared to the control strain) were selected and further analyzed for β-galactosidase activity. Genes identified to contain transposon insertions that altered the β-galactosidase activity of EC958*fimE::lacZ* or EC958*fimX::lacZ* are listed in Tables 3 and 4, respectively. Strikingly, multiple independent mutants containing insertions in the *guaB* gene were identified for both EC958*fimE::lacZ* and EC958*fimX::lacZ*; thus the remainder of this study focused on understanding the regulatory role of *guaB* on *fimE* and *fimX* transcription.

292

293 *Deletion of guaB in EC958 leads to up-regulation of the fimE and fimX recombinase genes but*
294 *slower fimS 'on' switching*

295 In order to study how *guaB* regulates *fimE* and *fimX*, we constructed defined deletion mutants in
296 EC958*fimE*::*lacZ* and EC958*fimX*::*lacZ* to generate the following strains: EC958*fimE*::*lacZ guaB*
297 and EC958*fimX*::*lacZ guaB*. Activity from the *fimE* and *fimX* promoters was measured by
298 determining the β-galactosidase activity from control and *guaB* mutant strains (Fig. 8A, B).
299 Deletion of *guaB* resulted in significantly increased promoter activity from both
300 EC958*fimE*::*lacZ guaB* (2-fold, $P<0.05$, Fig. 8A) and EC958*fimX*::*lacZ guaB* (1.5-fold, $P<0.05$,
301 Fig. 8B). Furthermore, complementation of the mutant strains by over-expressing *guaB in trans*
302 (via plasmid pGuaB) resulted in promoter activity comparable to the parental controls. These
303 results strongly suggest that the *guaB* gene product contributes to the regulation of *fimE* and *fimX*
304 in EC958.

305

306 To further assess the effect of *guaB* on *fimS* inversion, we generated an EC958*guaB* mutant and
307 determined its switching profile using DISCus. Static subculture of EC958 and EC958*guaB* was
308 performed over a 5-day period as described in previous sections. DISCus analysis of *fimS* was
309 performed on samples at days 1, 3 and 5. Analysis of samples taken at days 3 and 5 revealed a
310 significantly slower 'on' switching profile for EC958*guaB* compared to EC958 (Fig. 8C).
311 Furthermore, this slower *fimS* switching rate was restored to wild-type level following
312 complementation of EC958*guaB* with plasmid pGuaB (Fig. 8C). Taken together, this data
313 strongly supports a role for the *guaB* gene in *fimS* inversion.

314

The effect of guaB deletion on fimE and fimX transcription is partially dependent on GTP homeostasis and mimics (p)ppGpp stress response conditions

Guanosine tetra- and pentaphosphate, also known as (p)ppGpp, is a stress response alarmone that has been shown to increase type 1 fimbriae expression by up-regulating *fimB* and to a lesser extent, *fimE* transcription in *E. coli* (36). GuaB catalyzes the rate-limiting step in GMP biosynthesis and its deletion depletes the intracellular GTP pool (37, 38). Production of large amounts of (p)ppGpp can also result in a sharp decline in the intracellular GTP level both by direct GTP consumption and by (p)ppGpp-mediated GuaB inhibition (38, 39). Thus, (p)ppGpp is involved in regulating intracellular GTP homeostasis (38).

We hypothesized that the effect of *guaB* deletion on *fimE* and *fimX* transcription in EC958 may be mediated through (p)ppGpp and tested this using pooled human urine as a growth medium. We predicted that *guaB* deletion would induce the stringent response as a result of reduced cellular GTP and trigger (p)ppGpp production by the action of purine salvage pathways (40) utilizing guanine and guanosine species present in human urine (41, 42). Elevated levels of (p)ppGpp, in turn, would cause increased transcription of *fimE* and *fimX*. To test this, we first used a sub-inhibitory concentration of serine hydroxamate (SHX, 0.2 mM) to induce (p)ppGpp generation within the cell via depletion of serine-charged t-RNA, leading to activation of the amino acid starvation pathway (43). Stationary phase cultures of EC958*fimE*::*lacZ* and EC958*fimX*::*lacZ* grown in the presence or absence of SHX were analyzed for β-galactosidase activity (Fig. 9). The addition of SHX led to a significant de-repression of the *fimE* promoter (Fig. 9A; $P<0.05$), albeit not to the level seen in EC958*fimE*::*lacZ guaB*. No significant change was observed in *fimX* promoter activity (Fig. 9B).

Next, we attempted to replenish the depleted intracellular GTP pool in *guaB* deletion reporter strains by direct supplementation with GTP. The rationale behind this was that restoring intracellular GTP levels would rescue the cell from stress, leading to a decline in (p)ppGpp production and a subsequent decrease in *fimE* and *fimX* transcription. Thus, EC958*fimE*::*lacZ guaB* and EC958*fimX*::*lacZ guaB* were grown in pooled human urine supplemented with 0.5 mM GTP. For both strains, the addition of GTP led to a significant decrease in *fimE* ($P<0.01$) and *fimX* ($P<0.05$) promoter activities to levels similar to those observed in the parent EC958*fimE*::*lacZ* (Fig. 9C) and EC958*fimX*::*lacZ* strains (Fig. 9D). Taken together, these results suggest that GTP depletion in a *guaB* mutant background mimics conditions observed during (p)ppGpp stress and is at least partially responsible for increased transcription of *fimE* and *fimX*.

The guaB gene is required for EC958 persistence in urine and bladder colonization in a mouse UTI model

In order to assess the contribution of *guaB* to the virulence of EC958, we tested the ability of the EC958*guaB* mutant to survive in the mouse urinary tract using a competitive infection assay. We employed an EC958*lac* strain as the wild-type to enable differentiation of both strains on MacConkey lactose medium; EC958*lac* colonized the mouse bladder in equivalent numbers to wild-type EC958 in a mixed competitive infection (Supporting Information Fig. S4A, B). EC958*lac* and EC958*guaB* inocula were prepared by four successive rounds of static subculture in LB broth (3x48 hours followed by 1x24 hours); under these conditions both strains expressed similar levels of type 1 fimbriae (Supporting Information Fig. S4C). Female C57BL/6 mice were co-inoculated with 1:1 ratio of EC958*lac* and EC958*guaB*, and the colonization of each strain

was assessed at 24 hours post infection. In these experiments, EC958*guaB* was significantly outcompeted by EC958*lac* in the bladder ($P<0.01$) and urine ($P<0.05$) of infected mice (Fig. 10).

Discussion

The emergence and rapid spread of the UPEC ST131 clone has been well documented since 2008 with epidemiological reports from all over the world. Like other UPEC, *E. coli* ST131 strains utilize type 1 fimbriae for colonization of the urinary tract. However, most ST131 isolates from the globally predominant clade C sub-lineage possess an IS*Ec55* insertion element within the tyrosine-like recombinase *fimB* gene that is associated with reduced type 1 fimbriae expression (8, 28). Here, we define the molecular basis of *fimS* inversion in this clinically-relevant fluoroquinolone-resistant group of *E. coli* ST131 strains.

The high prevalence of the *fimB*::IS*Ec55* insertion in ST131 strains from clade C led us to assess the impact of this insertion on type 1 fimbriae expression. We have previously reported a delayed 'on' switching phenotype of type 1 fimbriae expression in a subset of the strains used in the current study (8). We therefore compared the type 1 fimbriae expression profile of a large collection of ST131 strains that possessed an intact or disrupted *fimB* gene over multiple rounds of static subculture. Overall, in accordance with previous observations (8), most ST131 strains containing the *fimB*::IS*Ec55* insertion were able to express type 1 fimbriae, but exhibited a slower 'off' to 'on' switching profile during static growth. Interestingly, in the present analysis, six strains were unable to express type 1 fimbriae after prolonged subculture, suggesting they lack the capacity to make functional type 1 fimbriae. Two of these strains had large deletions in the *fim* operon and transformation of the remaining four strains with a plasmid containing *fimB* induced type 1 fimbriae expression in only one strain. All three remaining strains harboured the *fimX* recombinase gene previously reported to switch *fimS* 'on' (24), indicating that they may contain other mutations that disrupt this phenotype.

387

388 The presence of the IS*Ec55* insertion element in *fimB* was associated with increased transcription
389 of the downstream *fimE* gene in the clade C representative EC958 strain and four other clade C
390 ST131 strains. Mapping of the *fimE* promoter in these strains revealed that IS*Ec55* did not
391 contain an independent promoter driving *fimE* transcription. However, we did observe that
392 deletion of H-NS, a global transcriptional regulator and a known repressor of *fimE* (35), did not
393 have a major effect on *fimE* transcription in EC958. H-NS is known to bind preferentially to
394 intrinsically-curved DNA and AT-rich sequences, usually found in promoter regions, to exert
395 regulatory effects on its many target genes (44, 45). Our observations indicate an *in trans* effect
396 of IS*Ec55* that could alter the local DNA structure and inhibit H-NS binding. Indeed, analogous
397 alterations in the transcription of genes adjacent to other insertion elements have been
398 documented in *E. coli* (46-48).

399

400 Analysis of *E. coli* ST131 genomes has revealed that the *fim* region is associated with
401 recombination (7, 28). Here, we provide a comprehensive analysis of type 1 fimbriae regulation
402 in fluoroquinolone-resistant clade C ST131 strains that contain the *fimB*::IS*Ec55* insertion. The
403 expression of type 1 fimbriae by the majority of ST131 strains containing the *fimB*::IS*Ec55*
404 insertion suggested that they possess an alternative recombinase/s capable of *fimS* inversion.
405 Using a combined mutagenesis and complementation strategy, we showed that both FimE and
406 FimX could mediate *fimS* inversion in EC958, with FimE demonstrating the greatest *fimS*
407 inversion activity under the static growth conditions employed in this study. We did not observe
408 any significant difference in *fimX* transcript levels in ST131 strains with an intact *fimB* and those
409 with the *fimB*::IS*Ec55* insertion. We also developed DISCus, a novel read-mapping approach

based on Illumina sequencing, to quantitatively determine the percentage of *fimS* 'on' or 'off' populations. Our data suggest that *fimE* plays a more important role than *fimX* in regulating the orientation of *fimS* during *in vitro* culture. This is in agreement with a previous report that detected relatively low levels of FimX activity *in vitro*, but observed rapid expression of type 1 fimbriae upon experimental infection in strains with FimX as the only active recombinase (25). The role of FimX in the inversion of *fimS* in EC958 during *in vivo* infection remains to be elucidated. In this respect, DISCus could be used to monitor *fimS* orientation in such populations. We also note that DISCus could be applied more broadly to analyze DNA invertible elements in other bacteria.

To identify potential regulators of the *fimE* and *fimX* genes in EC958, we employed random transposon mutagenesis of the *fimE* and *fimX* reporter strains and identified several genes that when mutated caused increased activity of the *fimE* and *fimX* promoters. The *guaB* gene, which encodes an enzyme that catalyzes the first rate limiting step in *de novo* GTP/GDP biosynthesis and is responsible for maintaining GTP homeostasis (49), was identified in screens of both reporter strains and was the focus of subsequent experimental analysis (see below). Mutation of several other genes was also linked with increased *fimE* promoter activity (*yubO, pdxH, lrhA, dprA*) or increased *fimX* promoter activity (*betA, yjjA*). The LysR family transcriptional regulator *lrhA* has previously been shown to repress both *fimB* and *fimE* (50), and our identification of *lrhA* in this study as a repressor of *fimE* is consistent with these results. The *yubO* gene is located on a 135.6 kb IncF plasmid in EC958 and encodes a protein of unknown function (51). Three independent Tn*5* mutants were identified in *yubO*, however specific mutagenesis of *yubO* failed to reproduce a significant increase in *fimE* transcription (data not shown). Thus, a definite role

433 for *yubO* in type 1 fimbriae regulation remains to be demonstrated. The *dprA* gene encodes a
434 putative DNA processing protein implicated in natural bacterial transformation (52) and has been
435 previously reported to be expressed *in vivo* during UTI (53). However, the molecular mechanism
436 by which *dprA* might affect *fimE* transcription, as well as the role of *pdxH* (encodes an enzyme
437 required for vitamin B6 biosynthesis (54)), *betA* (encodes a choline dehydrogenase (55)) and *yjjA*
438 (encodes a putative metal chaperone) in type 1 fimbriae expression, remains to be determined.
439
440 We focused our molecular investigation on the role of the *guaB* gene in *fimE* and *fimX*
441 regulation. While there is no direct link between *guaB* and expression of type 1 fimbriae in the
442 literature, *guaB* has been shown to be upregulated in women with UTI (53) and is important for
443 UPEC fitness in an experimental model of systemic infection (56). In other studies, the (p)ppGpp
444 alarmone, synthesized from GTP, has been shown to increase type 1 fimbriae expression in
445 *E. coli* (36). Strains lacking any (p)ppGpp exhibit reduced transcription from the *fimB* and *fimE*
446 promoters, although the effect on the latter gene is approximately half of that reported for *fimB*
447 (36). Under conditions of nutritional stress, (p)ppGpp controls global metabolic changes within
448 the cell (57-59) via direct interaction with RNA polymerase (60, 61) and activation of stress-
449 associated sigma factors (57). Synthesis of (p)ppGpp results in a reduction of the intracellular
450 GTP pool (62-64). Recently, it has been reported that (p)ppGpp directly inhibits various GTP
451 biosynthesis enzymes, thus further lowering the level of cellular GTP (38). We hypothesized that
452 deletion of *guaB* would produce a GTP deficient state mimicking that observed during the
453 activation of the stringent response pathway, and that this in turn would increase *fimE* and *fimX*
454 promoter activity. Chemical induction of this pathway in EC958 increased *fimE* promoter
455 activity and the addition of GTP to the culture media of *guaB* mutant strains significantly

456 reduced both *fimE* and *fimX* promoter activity. Taken together, these data support the hypothesis
457 that the cellular GTP concentration influences type 1 fimbriae expression by controlling the
458 transcription of *fimE* and *fimX*. We suggest that this effect is partly mediated by the action of the
459 (p)ppGpp alarmone on *fimE* promoter activity in strains that lack a functional copy of the *fimB*
460 gene. Indeed, DISCus analysis of EC958*guaB* revealed an overall slower *fimS* 'on' switching
461 phenotype compared to the wild-type EC958, possibly due to the strong natural bias for FimE to
462 mediate 'on' to 'off' switching (14, 65). These findings are also consistent with our mouse
463 colonization data, which showed that an EC958*guaB* mutant was significantly outcompeted by
464 wild-type EC958 with respect to bladder colonization and persistence in urine.
465
466 In conclusion, this work has identified and characterized several novel molecular mechanisms
467 associated with the regulation of type 1 fimbriae in *E. coli* ST131 strains that harbour an IS*Ec55*
468 insertion in the *fimB* recombinase gene. Our data demonstrate that type 1 fimbriae regulation in
469 these strains is different to that described for non-ST131 UPEC, highlighting the importance of
470 understanding the control of this essential virulence factor in the context of a clinically dominant
471 MDR resistant clone. Overall, the impact of this mutation on the fitness and global dissemination
472 of ST131 remains to be determined. However, given that the only non-ST131 strain shown to
473 harbour the *fimB*::IS*Ec55* insertion to date is the probiotic Nissle 1917 strain (8), it is tempting to
474 speculate that such modulation of type 1 fimbriae expression may be associated with enhanced
475 colonization of the gut.
476

Experimental Procedures

Ethics statement

Approval for mouse infection studies was obtained from the University of Queensland Animal Ethics Committee (SCMB/471/09/NHMRC (NF)). Experiments were carried out in strict accordance with the recommendations in the Animal Care and Protection Act (Queensland, 2002) and the Australian Code of Practice for the Care and Use of Animals for Scientific Purposes (8th edition, 2013). Approval for the collection of human urine was obtained from the University of Queensland Institutional Human Research Ethics Committee (2015000347) and the Griffith University Human Ethics Research Committee (MSC/06/08/HREC). Participation was voluntary and all individuals provided informed consent prior to participation in the study.

Bacterial strains and growth conditions

The *E. coli* strains and plasmids used in this study are listed in Table S1 in the Supporting Information. *E. coli* EC958 is a completely sequenced fluoroquinolone-resistant Clade C ST131 strain originally isolated in the United Kingdom in 2005 (7, 8, 29). Other *E. coli* ST131 strains were isolated from urine samples collected at hospitals in Manchester and Preston, Northwest England (n=54) and Brisbane, Australia (n=37). Most of the isolates (n=71) used in the present study have been described previously (7, 8, 29, 66-68). The additional 21 strains were collected from Brisbane, Australia as part of routine methods for UTI diagnosis. Strains were routinely cultured at 37°C on solid or in liquid lysogeny broth (LB) unless otherwise specified. Culture media was supplemented with appropriate antibiotics as required: gentamicin (Gent, 20 μg ml^{-1}), chloramphenicol (Cm, 30 μg ml^{-1}). Human urine, when used as culture media, was pooled from at least three healthy donors with no recent history of antibiotic use.

DNA manipulations and genetic techniques

Chromosomal DNA purification, PCR and DNA sequencing was performed as previously described (69). PCR screening for the presence of *fimH* (70) and the insertion element within *fimB* was performed as previously reported (8). The sequence type of UTI isolates used in this study was determined by multilocus sequence typing as previously described (4, 66, 67). DNA extraction for Illumina sequencing was performed using the Ultraclean® Microbial DNA Isolation Kit (MO BIO Laboratories). Restriction enzymes were purchased from New England Biolabs (Genesearch, Australia). All mutants, tagged strains and plasmid constructs were confirmed by PCR followed by Sanger sequencing performed at the Australian Equine Genetics Research Centre (Queensland, Australia). Illumina sequencing was performed at the Australian Genome Research Facility (Melbourne, Australia).

Construction of plasmids

The plasmids used for *in trans* complementation were created by PCR amplification of the respective gene from EC958 (*fimB* was amplified from CFT073) using primers listed in Supporting Information Table S1. Relevant PCR products were digested with SacI-HindIII and ligated into SacI-HindIII-digested pSU2718 (71). The cloned genes were under the control of a *lac* promoter; cloned genes were induced by the addition of 1 mM IPTG (Sigma Aldrich) to the culture medium.

Construction of deletion mutants and complemented strains

522 EC958 mutants were constructed using λ-Red mediated homologous recombination as
523 previously described (8) using primers listed in Table S1. A three-step PCR procedure was
524 employed for the generation of products with 500 bp homology regions used in recombination
525 (72). Plasmid pCP20 (73) was modified by the introduction of a gentamicin resistance cassette at
526 the NcoI site to yield pCP20-Gent. For complementation of mutants, removal of the FRT-site-
527 flanked chloramphenicol cassette was mediated by the Flp recombinase expressed by pCP20-
528 Gent. Mutant strains were then complemented by introduction of the respective genes cloned into
529 the low-copy number pSU2718 plasmid. All *lacZ* reporter-tagged transcriptional fusions were
530 generated in an *mKate2*-tagged EC958*lac* background using PCR products with a *lacZ-Cm*
531 cassette flanked by 500 bp homology regions specific to *fimE* or *fimX*.
532
533 *Type 1 fimbriae expression profile*
534 A type 1 fimbriae expression profile was established for all 91 *E. coli* ST131 strains examined in
535 this study. Strains were grown overnight on LB agar, and single colonies were picked and used
536 to inoculate a 5 ml LB for overnight aerobic (shaking) growth. A volume of 1 µl of each
537 overnight culture was inoculated into a new tube containing 5 ml LB and cultured for 24 hours
538 under static conditions. Strains were sub-cultured from the air-liquid interface in a similar
539 manner for further growth. Type 1 fimbriae expression was determined at each stage of
540 subculture using a yeast cell agglutination assay as previously described (8). Type 1 fimbriae
541 expression of EC958 wild-type and mutant derivatives was monitored similarly. The orientation
542 of *fimS* was evaluated from single colonies by PCR as previously described with primers 2848,
543 2859 and 2850 listed in Table S1 (24). Cells from colonies with *fimS* in the 'off' orientation were
544 used to inoculate 5 ml LB broth and cultured for 24 hours under static conditions; a volume of 10

µl was taken from the air-liquid interface and used to generate a new subculture every 24 hours over a 5-day period. For each subculture, type 1 fimbriae expression was monitored by yeast cell agglutination and western blot analysis of whole cell lysates using a FimA-specific antibody. A volume of 1 ml was also collected from the air-liquid interface at each 24-hour time point; cells were pelleted by centrifugation, genomic DNA was extracted and sequenced using Illumina technology for DISCus analysis.

RNA isolation, cDNA synthesis and quantitative RT-PCR (qRT-PCR) analysis

RNA was extracted from bacteria grown aerobically at 37°C in M9 minimal medium supplemented with 0.2% glucose (w/v) (74). Mid-log phase cultures were standardized to OD_{600} = 0.6 prior to RNA extraction using the RNeasy Protect Bacteria Mini Kit (Qiagen) following the manufacturer's guidelines. RNA was treated with RNase-free DNase I to remove contaminating DNA and re-purified using Qiagen RNeasy columns. RNA samples were quantified spectrophotometrically at 260nm. cDNA synthesis was performed with 1 µg total RNA and random hexamer primers using the SuperScript®III First Strand Synthesis System (Life Technologies) according to the manufacturer's instructions. All cDNA samples were diluted 10-fold prior to semi-quantitative real time PCR (qRT-PCR) analysis. qRT-PCR reactions were performed using SYBR® Green Master Mix (Applied Biosystems) and 500 nM gene specific primers for *fimE*, *fimX* and *gapA* (Supporting Information Table S1) on a ViiA™ 7 instrument (Life technologies) with the following cycling parameters: initial denaturation at 95°C for 10 min followed by 40 cycles of denaturation at 95°C for 15 s, annealing at 60°C for 15 s and elongation at 72°C for 30 s. Each reaction was performed in quadruplicate. Amplicon specificity was confirmed via gel and melting curve analysis. The ViiA™ 7 software determined the threshold

cycle (C_t) for each reaction. The expression of *fimE* and *fimX* was normalized to *gapA* expression for each sample and the $2^{-\Delta\Delta Ct}$ method (75) was employed to calculate the difference in expression of the *fim* recombinase genes between strains with an intact *fimB* and those with a *fimB*::IS*Ec55* insertion.

Rapid amplification of cDNA ends (5' RACE)

The transcription start site (TSS) of *fimE* was mapped using the 5' RACE system (Life Technologies) according to manufacturer's guidelines. Briefly, total RNA was isolated as described above and first strand cDNA synthesis was performed using SuperScript™ II and a gene-specific primer (Supporting Information Table S1, primer 4342). The resulting cDNA was purified and a homopolymeric tail was added to its 3'-end using TdT and dCTP. The cDNA was then amplified by PCR using an anchor primer (supplied) and a gene-specific primer (Supporting Information Table S1, primer 4343) followed by another round of nested PCR (primer 4344). The purified PCR product was then sequenced to determine the TSS.

Sequence analysis of fimE

Nucleotide sequences of ST131 *fimE* promoter and coding regions (1074 bp) were obtained from previously published genomes of strains used in this study (n=26) (7). The corresponding sequences from two reference non-ST131 UPEC strains, UTI89 (GI: 91209055) and CFT073 (GI: 26111730) and the *E. coli* K-12 strain MG1655 (GI: 556503834) were included for comparison. Multiple sequence alignment was performed using Clustal X v2.0 (76) to construct a neighbour-joining phylogenetic tree which was then visualised with FigTree v1.4.2

590 [http://tree.bio.ed.ac.uk/software/figtree/]. Amino acid sequences of the FimE protein (198 AA)
591 were also aligned using Clustal X2.
592
593 *Quantification of the fimS promoter switching frequency using DISCus*
594 To accurately measure invertible DNA switching, a read mapping approach was developed to
595 determine the frequency of Illumina sequence reads that mapped uniquely to the 'on' or 'off'
596 orientation of the *fimS* invertible switch. To determine the ratio of 'off' to 'on' mapped reads, a
597 pseudo-reference containing both *fimS* orientations and 1 kbp of flanking sequence was
598 constructed using the relevant sequence from EC958 (GI:641682562). An analogous approach
599 was taken to construct a pseudo-reference for the *hyxR* promoter region. Illumina 100 bp paired-
600 end reads from ST131 strains were then mapped to the pseudo-reference sequences using
601 Burrows-Wheeler Aligner (77), and inter-converted to SAM (Sequence Alignment/Map) and
602 BAM (Binary Alignment/Map) files using SAMtools where necessary (78). To ascertain the
603 number of reads overlapping the unique bordering regions of the 'off' and 'on' orientations, and
604 thereby their relative switching frequencies, Bedmaps was used to count reads overlapping 10 bp
605 pseudo-exons, which were created at both edges of the 'off' and 'on' orientations (79). The
606 number of paired-reads, which traversed these bordering regions, was also counted. This was
607 accomplished by assigning six regions in the pseudo-reference, corresponding to 'left flank',
608 'right flank' or 'switch region' for both the 'off' and 'on' orientation. Paired end read locations
609 were determined from the BAM file and counted if they were found to traverse from a 'switch
610 region' to either 'flank' for the 'off' or 'on' orientation respectively. Reads were not counted if
611 they were unpaired or traversed from an 'on' region to an 'off' region. Final read counts were
612 normalised as a percentage of total input reads to allow comparison between independent

samples. Python and Bash scripts for generating pseudo-reference sequences and automating DISCus, respectively, are available in a public repository at https://github.com/LeahRoberts/DISCus.

Transposon mutagenesis analysis

A mini Tn*5*-Cm transposon containing a chloramphenicol (*Cm*) cassette flanked by Tn*5* mosaic ends was PCR amplified from NotI-digested pKD3 plasmid with primers 2279 and 2280 (Supporting Information Table S1). The amplicon was phosphorylated using T4 polynucleotide kinase (New England Biolabs) and mixed with EZ-Tn5™ transposase (Epicenter Biotechnologies) to create transposomes according to the manufacturer's guidelines. Electrocompetent cells of EC958 *fimE* and *fimX* promoter-*lacZ* transcriptional fusion strains were prepared as previously described (80). Cells were electroporated with transposomes and after a 2 h recovery period in SOC, were spread on LB plates supplemented with Cm and 5-bromo-4-chloro-3-indolyl-D-galactoside (X-Gal). Approximately 50,000 to 60,000 Cm resistant mutants were obtained for each strain. Mutant colonies were visually screened for increased blue color intensity on X-Gal plates using the parental strains as controls. Selected mutants were further screened for *lacZ* expression by measurement of β-galactosidase activity. The transposon insertion site of mutants with altered β-galactosidase activity was determined using an arbitrary PCR (using primers 2209 and 1799; Supporting Information Table S1) followed by a nested PCR (using primers 2240 and 1801) and sequencing of the final amplicon. Mutation of the *guaB* gene in EC958*fimE*::*lacZ-cm* and EC958*fimE*::*lacZ-cm* was performed using λ-Red homologous recombination as described above.

β-Galactosidase assays

β-Galactosidase assays were performed essentially as previously described (81). Briefly, strains carrying *fimE* and *fimX* promoter-*lacZ* transcriptional fusions were grown overnight in pooled human urine alone or supplemented with 0.2 mM serine hydroxamate (SHX) or 0.5 mM GTP as indicated. Cultures were diluted in Z-buffer (60 mM Na_2HPO_4, 40 mM NaH_2PO_4, 50 mM β-mercaptoethanol, 10 mM KCl, 1 mM $MgSO_4$ at pH 7.0) followed by the addition of 0.004% SDS (w/v) and chloroform to permeabilize the cells. The samples were incubated at 28°C, and reactions were initiated by the addition of *ortho*-Nitrophenyl-β-D-galactopyranoside (ONPG). The reactions were stopped with the addition of Na_2CO_3 (300 mM). The enzymatic activity (expressed in Miller units) was assayed in quadruplicate for each strain by measuring the absorbance at 420 nm.

Mouse model of UTI

The C57BL/6 mouse model of ascending UTI was employed as previously described (69). All strains used in this experiment were enriched for type 1 fimbriae expression by three successive rounds of static growth in LB for 48 hours followed by one round of static growth for 24 hours for inoculum preparation. All strains were positive for type 1 fimbriae expression as determined by yeast cell agglutination and western blot analysis. Infections were performed as competitive assays; the inoculum contained 1:1 strain mixture of EC958 WT (*lac*$^-$ strain) and EC958*guaB*. Bacteria ($5x10^8$ CFU in 30 µl PBS) were injected transurethrally into female C57BL/6 mice (8-10 weeks). Urine was collected from mice 24 h post challenge, after which they were euthanized by cervical dislocation. Bacterial loads in urine and bladder were enumerated as colony forming

units (CFU) counts. The two strains were differentiated by colony colour on MacConkey plates: white (*lac*⁻ WT) or pink (EC958*guaB*).

Statistical Analysis

All statistical analyses were performed using the GraphPad Prism 6 software package. Significant associations between *fimB* status and type 1 fimbriae expression were investigated with the $\chi 2$ test. Statistical significance of fold-changes in *fimE* transcript levels between ST131 strains was determined using a two-tailed Mann Whitney test. The Wilcoxon matched pairs signed-rank test and repeated-measures one-way ANOVA with Dunnett's multiple comparisons test were used to analyse results from β-galactosidase assays. A Pearson's $\chi 2$ test with Yates' continuity correction was used to compare raw read counts generated by DISCus using RStudio (v0.98.501). The significance level was adjusted to 0.0167 (alpha = 0.05, Bonferroni adjusted for three pairwise comparisons). Data from mouse UTI experiments was analyzed using a two-tailed Wilcoxon matched pairs signed-rank test. In all instances, statistical significance was considered at $P<0.05$.

Acknowledgements

We thank Barbara Arnts and Kendall Hepple for technical assistance with the mouse UTI model. This work was supported by grants from the National Health and Medical Research Council (NHMRC) of Australia (APP1069370 and APP1067455). MAS is supported by an NHMRC Senior Research Fellowship (APP1106930), SAB is supported by an NHMRC Career Development Fellowship (APP1090456), MT is supported by an Australian Research Council

680 (ARC) Discovery Early Career Researcher Award (DE130101169) and GCU is supported by an
681 ARC Future Fellowship (FT110101048).

682

683

References

1. **Russo TA, Johnson JR.** 2003. Medical and economic impact of extraintestinal infections due to Escherichia coli: focus on an increasingly important endemic problem. Microbes Infect **5:**449-456.
2. **Flores-Mireles AL, Walker JN, Caparon M, Hultgren SJ.** 2015. Urinary tract infections: epidemiology, mechanisms of infection and treatment options. Nat Rev Microbiol **13:**269-284.
3. **Coque TM, Novais A, Carattoli A, Poirel L, Pitout J, Peixe L, Baquero F, Canton R, Nordmann P.** 2008. Dissemination of clonally related Escherichia coli strains expressing extended-spectrum beta-lactamase CTX-M-15. Emerg Infect Dis **14:**195-200.
4. **Lau SH, Kaufmann ME, Livermore DM, Woodford N, Willshaw GA, Cheasty T, Stamper K, Reddy S, Cheesbrough J, Bolton FJ, Fox AJ, Upton M.** 2008. UK epidemic Escherichia coli strains A-E, with CTX-M-15 beta-lactamase, all belong to the international O25:H4-ST131 clone. Journal of Antimicrobial Chemotherapy **62:**1241-1244.
5. **Nicolas-Chanoine MH, Blanco J, Leflon-Guibout V, Demarty R, Alonso MP, Canica MM, Park YJ, Lavigne JP, Pitout J, Johnson JR.** 2008. Intercontinental emergence of Escherichia coli clone O25 : H4-ST131 producing CTX-M-15. Journal of Antimicrobial Chemotherapy **61:**273-281.
6. **Price LB, Johnson JR, Aziz M, Clabots C, Johnston B, Tchesnokova V, Nordstrom L, Billig M, Chattopadhyay S, Stegger M, Andersen PS, Pearson T, Riddell K, Rogers P, Scholes D, Kahl B, Keim P, Sokurenko EV.** 2013. The epidemic of extended-spectrum-beta-lactamase-producing Escherichia coli ST131 is driven by a single highly pathogenic subclone, H30-Rx. MBio **4:**e00377-00313.
7. **Petty NK, Ben Zakour NL, Stanton-Cook M, Skippington E, Totsika M, Forde BM, Phan MD, Gomes Moriel D, Peters KM, Davies M, Rogers BA, Dougan G, Rodriguez-Bano J, Pascual A, Pitout JD, Upton M, Paterson DL, Walsh TR, Schembri MA, Beatson SA.** 2014. Global dissemination of a multidrug resistant Escherichia coli clone. Proc Natl Acad Sci U S A **111:**5694-5699.
8. **Totsika M, Beatson SA, Sarkar S, Phan MD, Petty NK, Bachmann N, Szubert M, Sidjabat HE, Paterson DL, Upton M, Schembri MA.** 2011. Insights into a multidrug resistant Escherichia coli pathogen of the globally disseminated ST131 lineage: genome analysis and virulence mechanisms. PLoS One **6:**e26578.
9. **Totsika M, Kostakioti M, Hannan TJ, Upton M, Beatson SA, Janetka JW, Hultgren SJ, Schembri MA.** 2013. A FimH inhibitor prevents acute bladder infection and treats chronic cystitis caused by multidrug-resistant uropathogenic Escherichia coli ST131. J Infect Dis **208:**921-928.
10. **Blomfield IC.** 2001. The regulation of pap and type 1 fimbriation in Escherichia coli. Adv Microb Physiol **45:**1-49.
11. **Klemm P, Jorgensen BJ, van Die I, de Ree H, Bergmans H.** 1985. The fim genes responsible for synthesis of type 1 fimbriae in Escherichia coli, cloning and genetic organization. Mol Gen Genet **199:**410-414.

12. **Abraham JM, Freitag CS, Clements JR, Eisenstein BI.** 1985. An invertible element of DNA controls phase variation of type 1 fimbriae of Escherichia coli. Proc Natl Acad Sci U S A **82:**5724-5727.
13. **Klemm P.** 1986. Two regulatory fim genes, fimB and fimE, control the phase variation of type 1 fimbriae in Escherichia coli. EMBO J **5:**1389-1393.
14. **Gally DL, Leathart J, Blomfield IC.** 1996. Interaction of FimB and FimE with the fim switch that controls the phase variation of type 1 fimbriae in Escherichia coli K-12. Mol Microbiol **21:**725-738.
15. **Stentebjerg-Olesen B, Chakraborty T, Klemm P.** 2000. FimE-catalyzed off-to-on inversion of the type 1 fimbrial phase switch and insertion sequence recruitment in an Escherichia coli K-12 fimB strain. FEMS Microbiol Lett **182:**319-325.
16. **Smith SG, Dorman CJ.** 1999. Functional analysis of the FimE integrase of Escherichia coli K-12: isolation of mutant derivatives with altered DNA inversion preferences. Mol Microbiol **34:**965-979.
17. **Olsen PB, Klemm P.** 1994. Localization of promoters in the fim gene cluster and the effect of H-NS on the transcription of fimB and fimE. FEMS Microbiol Lett **116:**95-100.
18. **Blomfield IC, Kulasekara DH, Eisenstein BI.** 1997. Integration host factor stimulates both FimB- and FimE-mediated site-specific DNA inversion that controls phase variation of type 1 fimbriae expression in Escherichia coli. Mol Microbiol **23:**705-717.
19. **Blomfield IC, Calie PJ, Eberhardt KJ, McClain MS, Eisenstein BI.** 1993. Lrp stimulates phase variation of type 1 fimbriation in Escherichia coli K-12. J Bacteriol **175:**27-36.
20. **Schwan WR.** 2011. Regulation of *fim* genes in uropathogenic *Escherichia coli*. World J Clin Infect Dis **1:**17-25.
21. **Old DC, Duguid JP.** 1970. Selective outgrowth of fimbriate bacteria in static liquid medium. J Bacteriol **103:**447-456.
22. **Hasman H, Schembri MA, Klemm P.** 2000. Antigen 43 and type 1 fimbriae determine colony morphology of Escherichia coli K-12. J Bacteriol **182:**1089-1095.
23. **Hung C, Zhou Y, Pinkner JS, Dodson KW, Crowley JR, Heuser J, Chapman MR, Hadjifrangiskou M, Henderson JP, Hultgren SJ.** 2013. Escherichia coli biofilms have an organized and complex extracellular matrix structure. MBio **4:**e00645-00613.
24. **Bryan A, Roesch P, Davis L, Moritz R, Pellett S, Welch RA.** 2006. Regulation of type 1 fimbriae by unlinked FimB- and FimE-like recombinases in uropathogenic Escherichia coli strain CFT073. Infect Immun **74:**1072-1083.
25. **Hannan TJ, Mysorekar IU, Chen SL, Walker JN, Jones JM, Pinkner JS, Hultgren SJ, Seed PC.** 2008. LeuX tRNA-dependent and -independent mechanisms of Escherichia coli pathogenesis in acute cystitis. Mol Microbiol **67:**116-128.
26. **Xie Y, Yao Y, Kolisnychenko V, Teng CH, Kim KS.** 2006. HbiF regulates type 1 fimbriation independently of FimB and FimE. Infect Immun **74:**4039-4047.
27. **Bateman SL, Seed PC.** 2012. Epigenetic regulation of the nitrosative stress response and intracellular macrophage survival by extraintestinal pathogenic Escherichia coli. Mol Microbiol **83:**908-925.

28. **Paul S, Linardopoulou EV, Billig M, Tchesnokova V, Price LB, Johnson JR, Chattopadhyay S, Sokurenko EV.** 2013. Role of homologous recombination in adaptive diversification of extraintestinal Escherichia coli. J Bacteriol **195:**231-242.
29. **Forde BM, Ben Zakour NL, Stanton-Cook M, Phan MD, Totsika M, Peters KM, Chan KG, Schembri MA, Upton M, Beatson SA.** 2014. The complete genome sequence of Escherichia coli EC958: a high quality reference sequence for the globally disseminated multidrug resistant E. coli O25b:H4-ST131 clone. PLoS One **9:**e104400.
30. **Schembri MA, Sokurenko EV, Klemm P.** 2000. Functional flexibility of the FimH adhesin: insights from a random mutant library. Infect Immun **68:**2638-2646.
31. **Gally DL, Rucker TJ, Blomfield IC.** 1994. The leucine-responsive regulatory protein binds to the fim switch to control phase variation of type 1 fimbrial expression in Escherichia coli K-12. J Bacteriol **176:**5665-5672.
32. **Bateman SL, Stapleton AE, Stamm WE, Hooton TM, Seed PC.** 2013. The Type 1 Pili Regulator Gene fimX and Pathogenicity Island PAI-X as Molecular Markers of Uropathogenic Escherichia coli. Microbiology doi:10.1099/mic.0.066472-0.
33. **Dorman CJ.** 2004. H-NS: a universal regulator for a dynamic genome. Nat Rev Microbiol **2:**391-400.
34. **Schembri MA, Olsen PB, Klemm P.** 1998. Orientation-dependent enhancement by H-NS of the activity of the type 1 fimbrial phase switch promoter in Escherichia coli. Mol Gen Genet **259:**336-344.
35. **Olsen PB, Schembri MA, Gally DL, Klemm P.** 1998. Differential temperature modulation by H-NS of the fimB and fimE recombinase genes which control the orientation of the type 1 fimbrial phase switch. FEMS Microbiol Lett **162:**17-23.
36. **Aberg A, Shingler V, Balsalobre C.** 2006. (p)ppGpp regulates type 1 fimbriation of Escherichia coli by modulating the expression of the site-specific recombinase FimB. Mol Microbiol **60:**1520-1533.
37. **Ochi K.** 1987. Metabolic initiation of differentiation and secondary metabolism by Streptomyces griseus: significance of the stringent response (ppGpp) and GTP content in relation to A factor. J Bacteriol **169:**3608-3616.
38. **Kriel A, Bittner AN, Kim SH, Liu K, Tehranchi AK, Zou WY, Rendon S, Chen R, Tu BP, Wang JD.** 2012. Direct regulation of GTP homeostasis by (p)ppGpp: a critical component of viability and stress resistance. Mol Cell **48:**231-241.
39. **Gallant J, Irr J, Cashel M.** 1971. The mechanism of amino acid control of guanylate and adenylate biosynthesis. J Biol Chem **246:**5812-5816.
40. **Vogels GD, Van der Drift C.** 1976. Degradation of purines and pyrimidines by microorganisms. Bacteriol Rev **40:**403-468.
41. **Sander G, Topp H, Wieland J, Heller-Schoch G, Schoch G.** 1986. Possible use of urinary modified RNA metabolites in the measurement of RNA turnover in the human body. Hum Nutr Clin Nutr **40:**103-118.
42. **Andreoli R, Manini P, De Palma G, Alinovi R, Goldoni M, Niessen WM, Mutti A.** 2010. Quantitative determination of urinary 8-oxo-7,8-dihydro-2'-deoxyguanosine, 8-oxo-7,8-dihydroguanine, 8-oxo-7,8-dihydroguanosine, and their non-oxidized forms: daily concentration profile in healthy volunteers. Biomarkers **15:**221-231.
43. **Shand RF, Blum PH, Mueller RD, Riggs DL, Artz SW.** 1989. Correlation between histidine operon expression and guanosine 5'-diphosphate-3'-diphosphate levels

during amino acid downshift in stringent and relaxed strains of Salmonella typhimurium. J Bacteriol **171:**737-743.

44. **Yamada H, Yoshida T, Tanaka K, Sasakawa C, Mizuno T.** 1991. Molecular analysis of the Escherichia coli hns gene encoding a DNA-binding protein, which preferentially recognizes curved DNA sequences. Mol Gen Genet **230:**332-336.
45. **Gordon BR, Li Y, Cote A, Weirauch MT, Ding P, Hughes TR, Navarre WW, Xia B, Liu J.** 2011. Structural basis for recognition of AT-rich DNA by unrelated xenogeneic silencing proteins. Proc Natl Acad Sci U S A **108:**10690-10695.
46. **Petersen C, Moller LB, Valentin-Hansen P.** 2002. The cryptic adenine deaminase gene of Escherichia coli. Silencing by the nucleoid-associated DNA-binding protein, H-NS, and activation by insertion elements. J Biol Chem **277:**31373-31380.
47. **Barker CS, Pruss BM, Matsumura P.** 2004. Increased motility of Escherichia coli by insertion sequence element integration into the regulatory region of the flhD operon. J Bacteriol **186:**7529-7537.
48. **Reynolds AE, Felton J, Wright A.** 1981. Insertion of DNA activates the cryptic bgl operon in E. coli K12. Nature **293:**625-629.
49. **Hedstrom L.** 2009. IMP dehydrogenase: structure, mechanism, and inhibition. Chem Rev **109:**2903-2928.
50. **Blumer C, Kleefeld A, Lehnen D, Heintz M, Dobrindt U, Nagy G, Michaelis K, Emody L, Polen T, Rachel R, Wendisch VF, Unden G.** 2005. Regulation of type 1 fimbriae synthesis and biofilm formation by the transcriptional regulator LrhA of Escherichia coli. Microbiology **151:**3287-3298.
51. **Phan MD, Forde BM, Peters KM, Sarkar S, Hancock S, Stanton-Cook M, Ben Zakour NL, Upton M, Beatson SA, Schembri MA.** 2015. Molecular Characterization of a Multidrug Resistance IncF Plasmid from the Globally Disseminated Escherichia coli ST131 Clone. PLoS One **10:**e0122369.
52. **Johnston C, Martin B, Fichant G, Polard P, Claverys JP.** 2014. Bacterial transformation: distribution, shared mechanisms and divergent control. Nat Rev Microbiol **12:**181-196.
53. **Hagan EC, Lloyd AL, Rasko DA, Faerber GJ, Mobley HL.** 2010. Escherichia coli global gene expression in urine from women with urinary tract infection. PLoS Pathog **6:**e1001187.
54. **Zhao G, Winkler ME.** 1995. Kinetic limitation and cellular amount of pyridoxine (pyridoxamine) 5'-phosphate oxidase of Escherichia coli K-12. J Bacteriol **177:**883-891.
55. **Styrvold OB, Falkenberg P, Landfald B, Eshoo MW, Bjornsen T, Strom AR.** 1986. Selection, mapping, and characterization of osmoregulatory mutants of Escherichia coli blocked in the choline-glycine betaine pathway. J Bacteriol **165:**856-863.
56. **Subashchandrabose S, Smith SN, Spurbeck RR, Kole MM, Mobley HL.** 2013. Genome-wide detection of fitness genes in uropathogenic Escherichia coli during systemic infection. PLoS Pathog **9:**e1003788.
57. **Paul BJ, Barker MM, Ross W, Schneider DA, Webb C, Foster JW, Gourse RL.** 2004. DksA: a critical component of the transcription initiation machinery that potentiates the regulation of rRNA promoters by ppGpp and the initiating NTP. Cell **118:**311-322.

58. **Barker MM, Gaal T, Josaitis CA, Gourse RL.** 2001. Mechanism of regulation of transcription initiation by ppGpp. I. Effects of ppGpp on transcription initiation in vivo and in vitro. J Mol Biol **305:**673-688.
59. **Murphy H, Cashel M.** 2003. Isolation of RNA polymerase suppressors of a (p)ppGpp deficiency. Methods Enzymol **371:**596-601.
60. **Chatterji D, Fujita N, Ishihama A.** 1998. The mediator for stringent control, ppGpp, binds to the beta-subunit of Escherichia coli RNA polymerase. Genes Cells **3:**279-287.
61. **Artsimovitch I, Patlan V, Sekine S, Vassylyeva MN, Hosaka T, Ochi K, Yokoyama S, Vassylyev DG.** 2004. Structural basis for transcription regulation by alarmone ppGpp. Cell **117:**299-310.
62. **Torok I, Kari C.** 1980. Accumulation of ppGpp in a relA mutant of Escherichia coli during amino acid starvation. J Biol Chem **255:**3838-3840.
63. **Johnson GS, Adler CR, Collins JJ, Court D.** 1979. Role of the spoT gene product and manganese ion in the metabolism of guanosine 5'-diphosphate 3'-diphosphate in Escherichia coli. J Biol Chem **254:**5483-5487.
64. **Lopez JM, Dromerick A, Freese E.** 1981. Response of guanosine 5'-triphosphate concentration to nutritional changes and its significance for Bacillus subtilis sporulation. J Bacteriol **146:**605-613.
65. **McClain MS, Blomfield IC, Eisenstein BI.** 1991. Roles of fimB and fimE in site-specific DNA inversion associated with phase variation of type 1 fimbriae in Escherichia coli. J Bacteriol **173:**5308-5314.
66. **Lau SH, Reddy S, Cheesbrough J, Bolton FJ, Willshaw G, Cheasty T, Fox AJ, Upton M.** 2008. Major uropathogenic Escherichia coli strain isolated in the northwest of England identified by multilocus sequence typing. Journal of Clinical Microbiology **46:**1076-1080.
67. **Sidjabat HE, Derrington P, Nimmo GR, Paterson DL.** 2010. Escherichia coli ST131 producing CTX-M-15 in Australia. Journal of Antimicrobial Chemotherapy **65:**1301-1303.
68. **Gibreel TM, Dodgson AR, Cheesbrough J, Fox AJ, Bolton FJ, Upton M.** 2012. Population structure, virulence potential and antibiotic susceptibility of uropathogenic Escherichia coli from Northwest England. J Antimicrob Chemother **67:**346-356.
69. **Allsopp LP, Totsika M, Tree JJ, Ulett GC, Mabbett AN, Wells TJ, Kobe B, Beatson SA, Schembri MA.** 2010. UpaH is a newly identified autotransporter protein that contributes to biofilm formation and bladder colonization by uropathogenic Escherichia coli CFT073. Infect Immun **78:**1659-1669.
70. **Johnson JR, Stell AL.** 2000. Extended virulence genotypes of Escherichia coli strains from patients with urosepsis in relation to phylogeny and host compromise. J Infect Dis **181:**261-272.
71. **Martinez E, Bartolome B, de la Cruz F.** 1988. pACYC184-derived cloning vectors containing the multiple cloning site and lacZ alpha reporter gene of pUC8/9 and pUC18/19 plasmids. Gene **68:**159-162.
72. **Derbise A, Lesic B, Dacheux D, Ghigo JM, Carniel E.** 2003. A rapid and simple method for inactivating chromosomal genes in Yersinia. FEMS Immunol Med Microbiol **38:**113-116.

73. **Cherepanov PP, Wackernagel W.** 1995. Gene disruption in Escherichia coli: TcR and KmR cassettes with the option of Flp-catalyzed excision of the antibiotic-resistance determinant. Gene **158:**9-14.
74. **Sambrook J, Fritsch EF, Maniatis T.** 1989. Molecular cloning: a laboratory manual, 2nd edition., 2 ed. Cold Spring Harbor Laboratory Press, Cold Spring Harbor, NY.
75. **Livak KJ, Schmittgen TD.** 2001. Analysis of relative gene expression data using real-time quantitative PCR and the 2(-Delta Delta C(T)) Method. Methods **25:**402-408.
76. **Larkin MA, Blackshields G, Brown NP, Chenna R, McGettigan PA, McWilliam H, Valentin F, Wallace IM, Wilm A, Lopez R, Thompson JD, Gibson TJ, Higgins DG.** 2007. Clustal W and Clustal X version 2.0. Bioinformatics **23:**2947-2948.
77. **Li H, Durbin R.** 2009. Fast and accurate short read alignment with Burrows-Wheeler transform. Bioinformatics **25:**1754-1760.
78. **Li H, Handsaker B, Wysoker A, Fennell T, Ruan J, Homer N, Marth G, Abecasis G, Durbin R.** 2009. The Sequence Alignment/Map format and SAMtools. Bioinformatics **25:**2078-2079.
79. **Neph S, Kuehn MS, Reynolds AP, Haugen E, Thurman RE, Johnson AK, Rynes E, Maurano MT, Vierstra J, Thomas S, Sandstrom R, Humbert R, Stamatoyannopoulos JA.** 2012. BEDOPS: high-performance genomic feature operations. Bioinformatics **28:**1919-1920.
80. **Langridge GC, Phan MD, Turner DJ, Perkins TT, Parts L, Haase J, Charles I, Maskell DJ, Peters SE, Dougan G, Wain J, Parkhill J, Turner AK.** 2009. Simultaneous assay of every Salmonella Typhi gene using one million transposon mutants. Genome Res **19:**2308-2316.
81. **Miller JH.** 1992. A short course in bacterial genetics: a laboratory manual and handbook for *Escherichia coli* and related bacteria, vol 1. Cold Spring Harbor Laboratory Press, Cold Spring Harbor, NY.
82. **Mobley HL, Green DM, Trifillis AL, Johnson DE, Chippendale GR, Lockatell CV, Jones BD, Warren JW.** 1990. Pyelonephritogenic Escherichia coli and killing of cultured human renal proximal tubular epithelial cells: role of hemolysin in some strains. Infect Immun **58:**1281-1289.
83. **Berger H, Hacker J, Juarez A, Hughes C, Goebel W.** 1982. Cloning of the chromosomal determinants encoding hemolysin production and mannose-resistant hemagglutination in Escherichia coli. J Bacteriol **152:**1241-1247.
84. **Mulvey MA, Schilling JD, Hultgren SJ.** 2001. Establishment of a persistent Escherichia coli reservoir during the acute phase of a bladder infection. Infect Immun **69:**4572-4579.
85. **Korhonen TK, Valtonen MV, Parkkinen J, Vaisanen-Rhen V, Finne J, Orskov F, Orskov I, Svenson SB, Makela PH.** 1985. Serotypes, hemolysin production, and receptor recognition of Escherichia coli strains associated with neonatal sepsis and meningitis. Infect Immun **48:**486-491.
86. **Allsopp LP, Beloin C, Ulett GC, Valle J, Totsika M, Sherlock O, Ghigo JM, Schembri MA.** 2012. Molecular characterization of UpaB and UpaC, two new autotransporter proteins of uropathogenic Escherichia coli CFT073. Infect Immun **80:**321-332.

87. **Phan MD, Peters KM, Sarkar S, Lukowski SW, Allsopp LP, Moriel DG, Achard ME, Totsika M, Marshall VM, Upton M, Beatson SA, Schembri MA.** 2013. The Serum Resistome of a Globally Disseminated Multidrug Resistant Uropathogenic Clone. PLoS Genet **9:**e1003834.
88. **Allsopp LP, Beloin C, Moriel DG, Totsika M, Ghigo JM, Schembri MA.** 2012. Functional heterogeneity of the UpaH autotransporter protein from uropathogenic Escherichia coli. J Bacteriol **194:**5769-5782.
89. **Chaveroche MK, Ghigo JM, d'Enfert C.** 2000. A rapid method for efficient gene replacement in the filamentous fungus Aspergillus nidulans. Nucleic Acids Res **28:**E97.

966 # Tables

967 **Table 1.** Type 1 fimbriae expression profile of *E. coli* ST131 strains

	Number of yeast agglutination positive ST131 strains following overnight growth in LB broth at 37°C (%)			
fimB Status	Shaking culture	Static subculture		
	Day 1	Day 1	Day 2	Day 3
fimB::IS*Ec55* (n=57)	8 (14)	27 (47.4)	34 (59.6)	52 (91.2)
Intact *fimB* (n=34)	24 (70.6)***	27 (79.4)*	27 (79.4)	29 (85.3)

968 *P<0.01, ***P<0.0001; $\chi 2$ test.

969

970

971 **Table 2.** Effect of FimB over-expression in type 1 fimbriae negative strains

Strain	*fimB* status	Genotype	*fimS* orientation	Yeast Agglutination*
S1	*fimB*::IS*Ec55*	Wild-type	OFF	-
		+ pFimB	ON	-
S18	*fimB*::IS*Ec55*	Wild-type	OFF	-
		+ pFimB	ON	+
S27	Intact	Wild-type	OFF	-
		+ pFimB	OFF	-
S61	*fimB*::IS*Ec55*	Wild-type	OFF	-
		+ pFimB	ON	-

972 *Yeast agglutination negative (-), positive (+)

973

974

975 **Table 3.** Mutated genes associated with increased *fimE* promoter activity

EC958 locus tag	Gene	Product	No. independent Tn*5* insertions	β-gal activity as Miller units[a] (mean±SD)	Fold-change relative to control[b] (mean±SD)
EC958_2815	*guaB*	inosine 5' monophosphate dehydrogenase	3	2102±56, 1321±28, 792±36	4.95±0.94 3.11±0.59 1.86±0.36
EC958_A0030	*yubO*	Unknown function, plasmid located	3	1175±139, 830±70, 702±40	2.76±0.61 1.95±0.40 1.65±0.32
EC958_1861	*pdxH*	pyridoxamine 5' phosphate oxidase	2	819±30, 1936±131	1.93±0.36 4.56±0.91
EC958_2624	*lrhA*	LysR homologue A	1	2348±365	5.52±1.35
EC958_3829	*dprA*	putative DNA processing protein	1	1358±59	3.20±0.62

976 SD, Standard deviation.

977 [a]Values represent data from each independently isolated Tn*5* mutant.

978 [b]β-gal activity of control strain EC958*fimE::lacZ* = 425±80.

979

980

981 **Table 4.** Mutated genes associated with increased *fimX* promoter activity

EC958 locus tag	Gene	Product	No. independent Tn*5* insertions	β-gal activity as Miller units (mean±SD)	Fold-change relative to control[a] (mean±SD)
EC958_2815	*guaB*	inosine 5' monophosphate dehydrogenase	1	94±7	1.52±0.15
EC958_0463	*betA*	choline dehydrogenase	1	108±9	1.74±0.18
EC958_0090	*yjjA*	putative metal chaperone	1	94±7	1.52±0.15

982 SD, Standard deviation.

983 [a]β-gal activity of control strain EC958*fimX::lacZ* = 62±4.

984

985 **Table 5.** Strains and plasmids used in this study

Strain[a]	Description	Reference
CFT073	Wild-type UPEC isolate	(82)
536	Wild-type UPEC isolate	(83)
UTI89	Wild-type UPEC isolate	(84)
IHE3034	Wild-type UPEC isolate	(85)
EC958	Wild-type UPEC isolate; *E. coli* ST131 ESBL	(8)
S1 pFimB	*E. coli* ST131 strain S1 pFimB, ESBL, Cm^r	This study
S18 pFimB	*E. coli* ST131 strain S18 pFimB, ESBL, Cm^r	This study
S27 pFimB	*E. coli* ST131 strain S27 pFimB, ESBL, Cm^r	This study
S61 pFimB	*E. coli* ST131 strain S61 pFimB, ESBL, Cm^r	This study
CFT973*hns*	CFT073*hns::kan*, Kan^r	(86)
536*hns*	536*hns::kan*, Kan^r	This study
UTI89*hns*	UTI89*hns::kan*, Kan^r	This study
IHE3034*hns*	IHE3034*hns::kan*, Kan^r	This study
EC958*hns*	EC958*hns::cm*, ESBL, Cm^r	(87)
MS3198	CFT073*lacIZ upaH*:*lacZ-zeo*	(88)
EC958 pKOBEG-Gent	EC958 pKOBEG-Gent, ESBL $Gent^r$	(8)
EC958*fimE*	EC958*fimE*::*cm*, ESBL Cm^r	This study
EC958*fimX*	EC958*fimX*::*cm*, ESBL Cm^r	This study
EC958*fimE fimX*	EC958*fimE fimX*::*cm*, ESBL Cm^r	This study
EC958*fimE fimX* pSU2718	EC958*fimE fimX*, ESBL Cm^r	This study
EC958*fimE fimX* pFimE	EC958*fimE fimX* pFimE, ESBL Cm^r	This study
EC958*fimE fimX* pFimX	EC958*fimE fimX* pFimX, ESBL Cm^r	This study
EC958*lac*::*mKate2*	EC958*lac*::*mKate2*::*cm*, ESBL Cm^r	(87)
EC958*fimE*::*lacZ-cm*	EC958*lac*::*mKate2* fimE::*lacZ-cm*, ESBL Cm^r	This study
EC958*fimX*::lacZ-*cm*	EC958*lac*::*mKate2 fimX*::*lacZ-cm*, ESBL Cm^r	This study
EC958*fimE*::*lacZ guaB*	EC958*lac*::*mKate2 fimE*::*lacZ guaB*::*cm*, ESBL Cm^r	This study

EC958*fimX*::*lacZ guaB*	EC958*lac*::*mKate2 fimX*::*lacZ guaB*::*cm*, ESBL Cm^r	This study
EC958*fimE*::*lacZ guaB* (pGuaB)	EC958*lac*::*mKate2 fimE*::*lacZ guaB*::*cm* pGuaB, ESBL Cm^r	This study
EC958*fimX*::*lacZ guaB* (pGuaB)	EC958*lac*::*mKate2 fimX*::*lacZ guaB*::*Cm* pGuaB, ESBL Cm^r	This study
Plasmid		
pKOBEG-Gent	λ-Red plasmid, replicates at 37°C, *araC* arabinose inducible promoter, Gent^r	(8, 89)
pCP20-Gent	Replicates at 30°C, encodes Flp recombinase, Gent^r	This study, (73)
pSU2718	Cloning vector, P*lac* promoter, replicates at 37°C, Cm^r	(71)
pFimB	pSU2718 *fimB*; *fimB* coding sequence from CFT073, Cm^r	This study
pFimE	pSU2718 *fimE*; *fimE* coding sequence from EC958, Cm^r	This study
pFimX	pSU2718 *fimX*; *fimX* coding sequence from EC958, Cm^r	This study
pGuaB	pSU2718 *guaB*; *guaB* coding sequence from EC958, Cm^r	This study

[a]In addition to the strains listed above, our *E. coli* ST131 strain collection comprised of 54 strains from the United Kingdom (S1-S54, including EC958; (7, 8, 29, 66, 68) and 37 strains from Australia (S55-S91; (7, 8, 67); Cm^r-chloramphenicol, Gent^r-gentamicin resistant, Kan^r-kanamycin resistant.

992 ## Figure Legends

993 **Fig. 1.** Schematic representation of the type 1 fimbrial operon. The 1895bp *fimB*::IS*Ec55*
994 insertion sequence element is depicted in its genomic context. CFT073, reference UPEC strain;
995 EC958, representative *E. coli* ST131 clade C strain; adapted from Totsika *et al.*(8).
996
997 **Fig. 2.** Quantification of *fimE* and *fimX* transcription in ST131 strains by qRT-PCR.
998 The level of *fimE* (A) and *fimX* (B) transcription relative to housekeeping gene *gapA* was
999 determined by qRT-PCR in mid-log phase ST131 strains with the *fimB*::IS*Ec55* insertion (n=5,
1000 including EC958) and compared to those with an intact *fimB* (n=4) to determine fold-difference
1001 in gene expression between the two groups using the $2^{-\Delta\Delta Ct}$ method. Bars represent group means
1002 ± standard deviation (SD). Asterisk indicates a statistically significant difference between the two
1003 groups ($P<0.05$) as determined by the two-tailed Mann Whitney test.
1004
1005 **Fig. 3.** Analysis of *fimE* promoter sequence.
1006 The transcription start site (TSS) of *fimE* was mapped by 5'RACE in EC958 and five other
1007 *E. coli* ST131 strains (S4, S54, S69, S88 and S90). Shown here is the consensus nucleotide
1008 sequence. The -35 and -10 promoter elements are underlined and the TSS mapped to a G residue
1009 164 bases upstream of the GTG start codon (indicated by the curved arrow).
1010
1011 **Fig. 4.** Contribution of FimE and FimX to *fimS* inversion and type 1 fimbriae expression in
1012 EC958.

Western blots demonstrating expression of the FimA major subunit protein of type 1 fimbriae using α-FimA antibody and yeast cell agglutination assays to monitor type 1 fimbriae expression (- negative, + positive fimbriae expression) in static cultures.

A. Type 1 fimbriae expression was measured in EC958 (wild-type), EC958*fimE*, EC958*fimX*, and EC958*fimE fimX* over 5 days of static subculture.

B. Type 1 fimbriae expression in EC958*fimE fimX* strains over 3 days of static subculture. EC958*fimE fimX* (pSU2718) was used as an empty vector control. Over-expression of FimE (pFimE) and FimX (pFimX) was induced by the addition of 1mM IPTG to the culture media.

Fig. 5. Quantification of *fimS* switch orientation bias in EC958 wild-type, mutants and complemented strains using DISCus.

A. *fimS* orientation in EC958, EC958*fimE*, EC958*fimX* and EC958*fimE fimX* over 5 days of static subculture quantified using DISCus. Samples from the air-liquid interface of each culture were taken on each day and used for genomic DNA extraction and Illumina sequencing. Bars represent *fimS* percentage 'on' population within each culture.

B. DISCus analysis of *fimS* orientation following *in trans* complementation with FimE (pFimE) or FimX (pFimE) in the EC958*fimE fimX* double mutant over 3 days of static subculture.

Fig. 6. Quantification of *fimX* switch orientation bias in EC958 wild-type, mutants and complemented strains using DISCus.

A. DISCus analysis of *fimX* switch orientation in EC958, EC958*fimE* and EC958*fimX* strains over 5 days of static subculture. Bars represent percentage *fimX* switch 'on' reads within each culture population.

1036 B. DISCus analysis of *fimX* switch orientation in EC958*fimE fimX* and in EC958*fimE fimX*
1037 following *in trans* complementation with FimE (pFimE) or FimX (pFimE) over 3 days of static
1038 subculture.
1039
1040 **Fig. 7.** Effect of *hns* deletion on *fimE* transcript level in different UPEC strains.
1041 A. Fold-change in *fimE* transcription in EC958*hns* compared to wild-type EC958 as determined
1042 by qRT-PCR.
1043 B-D. Fold-change in *fimE* transcription in non-ST131 wild-type UPEC strains and their
1044 corresponding *hns* deletion mutants, namely UTI89 (B), 536 (C) and IHE3034 (D) as determined
1045 by qRT-PCR. Vertical bars represent means±SD of three independent replicates.
1046
1047 **Fig. 8.** Effect of *guaB* deletion on *fimE*/*fimX* promoter activity and *fimS* switching in EC958.
1048 A-B. β-galactosidase activity of EC958 *fimE* (A) and *fimX* (B) promoter-*lacZ* reporter strains
1049 following overnight aerated growth in pooled human urine. All *guaB* mutant strains and
1050 complemented derivatives were constructed in their respective promoter-*lacZ* reporter
1051 backgrounds. Bars represent means ± SD of at least three independent biological experiments.
1052 Asterisk indicates a statistically significant difference ($P<0.05$) as determined by repeated-
1053 measures one-way ANOVA with Dunnett's multiple comparisons test.
1054 C. DISCus analysis of the effect of *guaB* deletion on *fimS* switching. EC958
1055 (wild-type), EC958*guaB* and EC958*guaB*(pGuaB) were grown statically in LB (37^{o}C) over a
1056 period of 5 days. Over-expression of GuaB in EC958*guaB*(pGuaB) was induced by the addition
1057 of 1mM IPTG. Genomic DNA was extracted after static subculture on days 1, 3 and 5, and
1058 Illumina sequencing data was analyzed by DISCus. Bars represent percentage 'on' reads of *fimS*

in each culture population. Asterisks indicate a statistically significant difference (* P = 0.01-0.001; *** $P < 0.0001$) as determined by a Pearson's $\chi 2$ test with Yates' continuity correction.

Fig. 9. Regulation of *fimE* and *fimX* promoter activity by (p)ppGpp.

A-B. Effect of serine hydroxamate (SHX, 0.2 mM) induced amino acid starvation on the promoter activity of *fimE* (A) and *fimX* (B) in EC958*fimE*:*lacZ* and EC958*fimX*:*lacZ* strains, respectively. All *guaB* mutant strains and complemented derivatives were constructed in their respective promoter-*lacZ* reporter backgrounds. Strains were incubated overnight under static conditions in pooled human urine and promoter activity was determined by the β-galactosidase assay. Bars represent means ± SD of three independent biological experiments with four technical replicates. Asterisk indicates a statistically significant difference (P<0.05) as determined by the Wilcoxon matched pairs signed-rank test.

C-D. Effect of GTP (0.5 mM) on the promoter activity of *fimE* (C) and *fimX* (D) in EC958*fimE*::*lacZ guaB* and EC958*fimX*::*lacZ guaB* strains, respectively. Asterisks indicate statistically significant differences (**P<0.01, *P<0.05) in *guaB* reporter strains upon addition of GTP, as determined by a repeated-measures one-way ANOVA with Dunnett's multiple comparisons test.

Fig. 10. Mouse urinary tract colonization by EC958 WT and EC958*guaB*. Female C57B/L6 mice were transurethrally inoculated with a 1:1 mixture of type 1 fimbriae enriched EC958 WT and EC958*guaB* strains in a competitive infection assay. Each marker represents total colony forming units (CFU) recovered from each mouse per 1 ml of urine or per 0.1 g of bladder tissue

(as labelled) on selective medium. Lines connect data points for the same mouse and horizontal bars represent median values. Asterisk indicates statistically significant difference between the strains for persistence in urine ($P<0.05$) as well as bladder colonization ($P<0.01$) as determined by the Wilcoxon matched pairs signed-rank test.

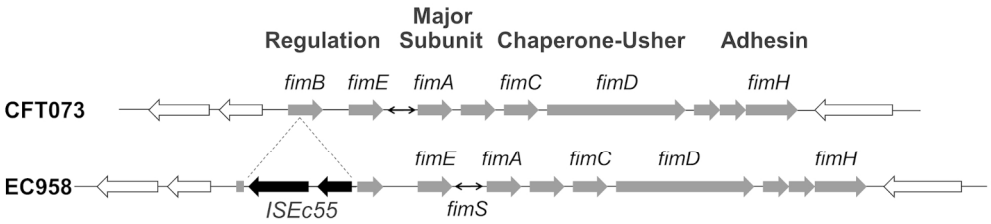

Fig. 1. Schematic representation of the type 1 fimbrial operon. The 1895bp fimB::ISEc55 insertion sequence element is depicted in its genomic context. CFT073, reference UPEC strain; EC958, representative E. coli ST131 clade C strain; adapted from Totsika et al.(8).
167x39mm (300 x 300 DPI)

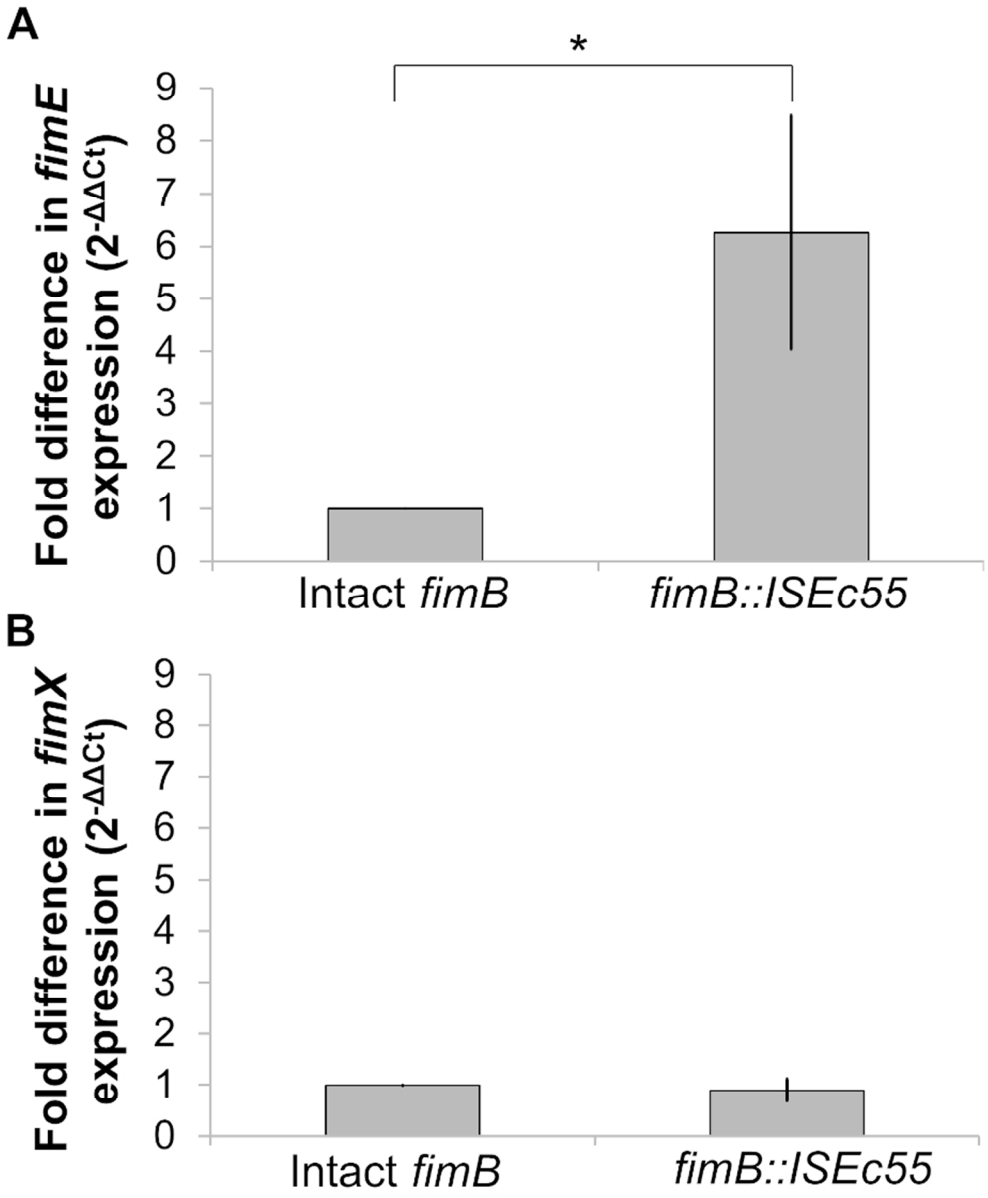

Fig. 2. Quantification of fimE and fimX transcription in ST131 strains by qRT-PCR.
The level of fimE (A) and fimX (B) transcription relative to housekeeping gene gapA was determined by qRT-PCR in mid-log phase ST131 strains with the fimB::ISEc55 insertion (n=5, including EC958) and compared to those with an intact fimB (n=4) to determine fold-difference in gene expression between the two groups using the 2-ΔΔCt method. Bars represent group means ± standard deviation (SD). Asterisk indicates a statistically significant difference between the two groups ($P<0.05$) as determined by the two-tailed Mann Whitney test.
78x95mm (300 x 300 DPI)

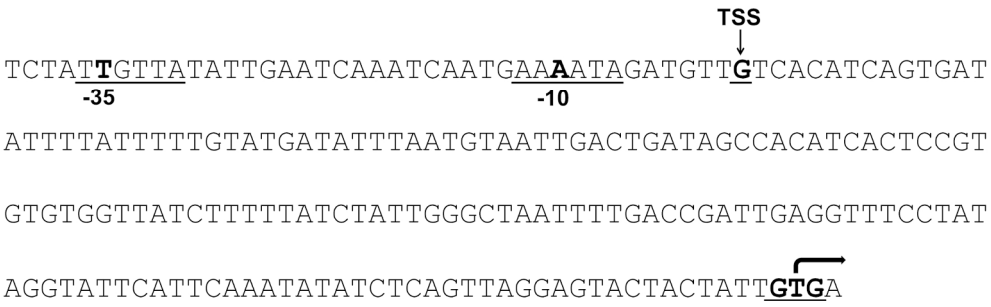

Fig. 3. Analysis of fimE promoter sequence. The transcription start site (TSS) of fimE was mapped by 5'RACE in EC958 and five other E. coli ST131 strains (S4, S54, S69, S88 and S90). Shown here is the consensus nucleotide sequence. The -35 and -10 promoter elements are underlined and the TSS mapped to a G residue 164 bases upstream of the GTG start codon (indicated by the curved arrow).
189x80mm (300 x 300 DPI)

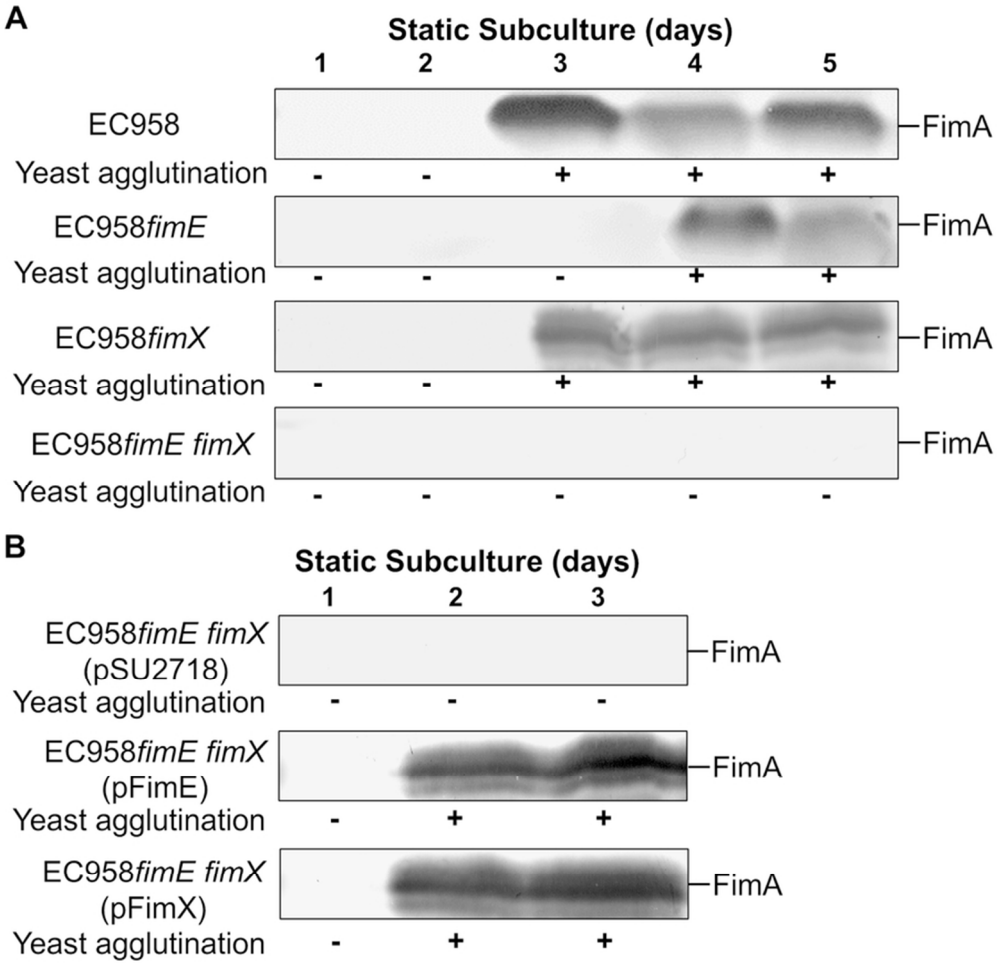

Fig. 4. Contribution of FimE and FimX to fimS inversion and type 1 fimbriae expression in EC958. Western blots demonstrating expression of the FimA major subunit protein of type 1 fimbriae using α-FimA antibody and yeast cell agglutination assays to monitor type 1 fimbriae expression (- negative, + positive fimbriae expression) in static cultures.

A. Type 1 fimbriae expression was measured in EC958 (wild-type), EC958fimE, EC958fimX, and EC958fimE fimX over 5 days of static subculture.

B. Type 1 fimbriae expression in EC958fimE fimX strains over 3 days of static subculture. EC958fimE fimX (pSU2718) was used as an empty vector control. Over-expression of FimE (pFimE) and FimX (pFimX) was induced by the addition of 1mM IPTG to the culture media.

76x74mm (300 x 300 DPI)

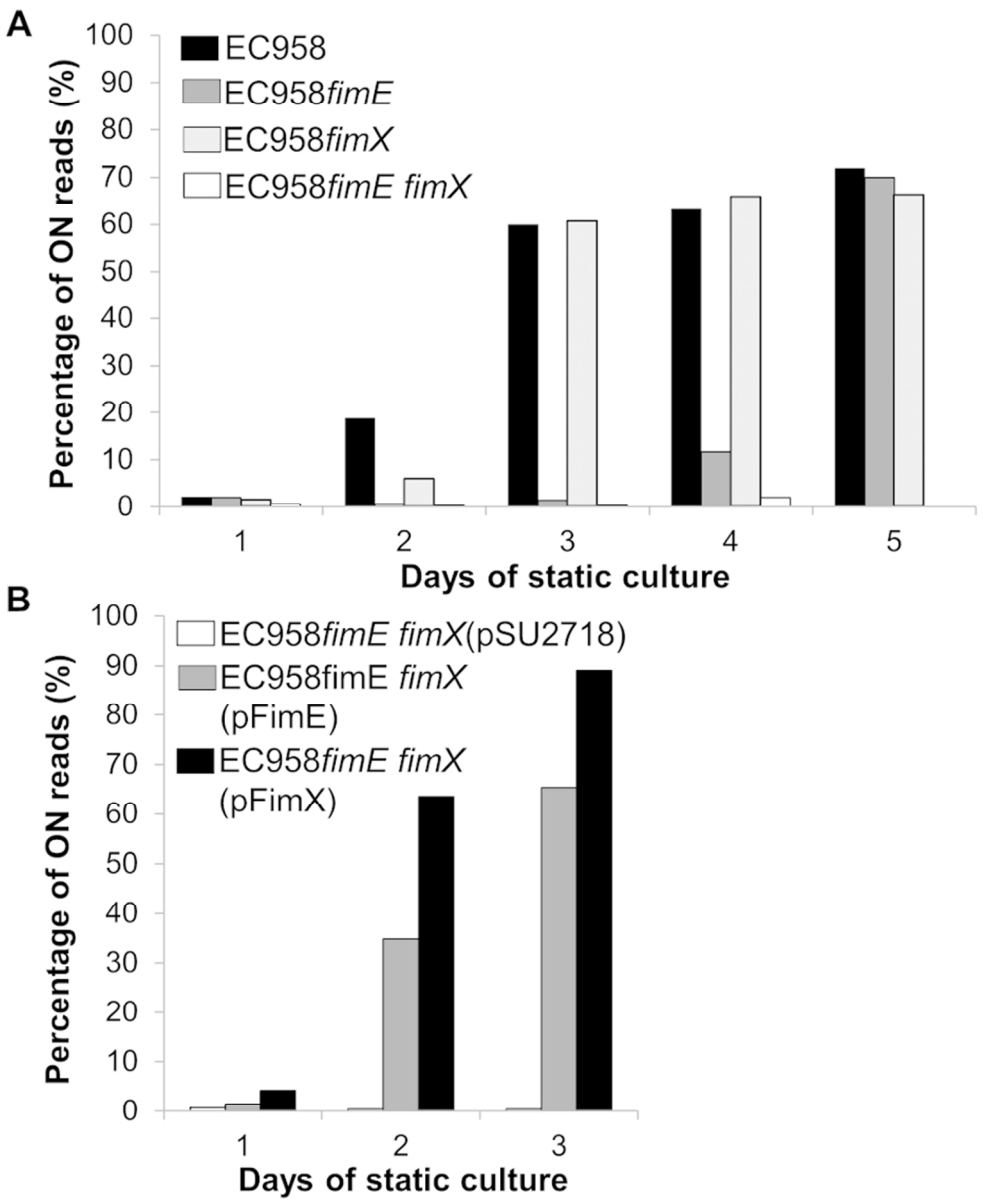

Fig. 5. Quantification of fimS switch orientation bias in EC958 wild-type, mutants and complemented strains using DISCus.

A. fimS orientation in EC958, EC958fimE, EC958fimX and EC958fimE fimX over 5 days of static subculture quantified using DISCus. Samples from the air-liquid interface of each culture were taken on each day and used for genomic DNA extraction and Illumina sequencing. Bars represent fimS percentage 'on' population within each culture.

B. DISCus analysis of fimS orientation following in trans complementation with FimE (pFimE) or FimX (pFimE) in the EC958fimE fimX double mutant over 3 days of static subculture.

78x96mm (300 x 300 DPI)

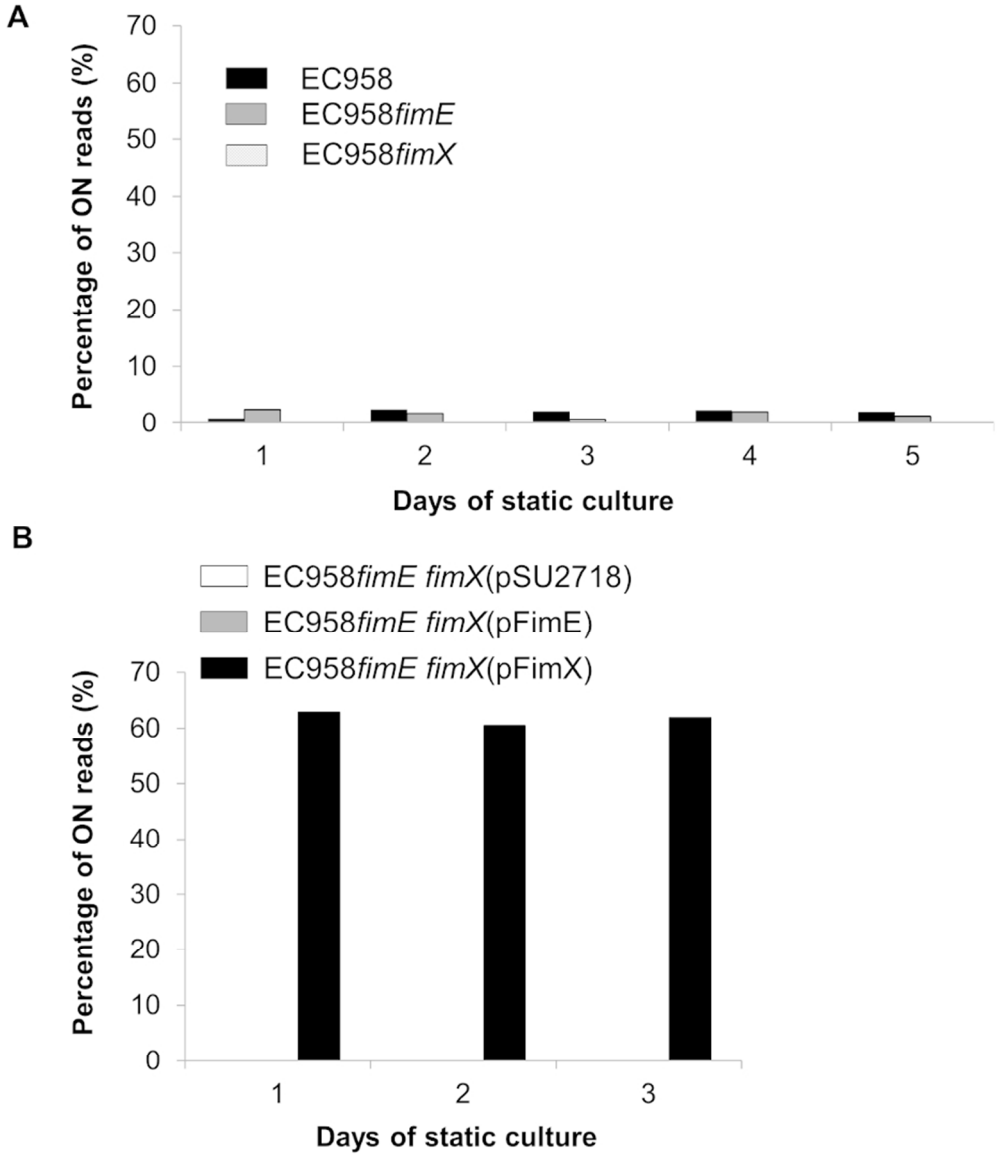

Fig. 6. Quantification of fimX switch orientation bias in EC958 wild-type, mutants and complemented strains using DISCus.
A. DISCus analysis of fimX switch orientation in EC958, EC958fimE and EC958fimX strains over 5 days of static subculture. Bars represent percentage fimX switch 'on' reads within each culture population.
B. DISCus analysis of fimX switch orientation in EC958fimE fimX and in EC958fimE fimX following in trans complementation with FimE (pFimE) or FimX (pFimE) over 3 days of static subculture.
78x91mm (300 x 300 DPI)

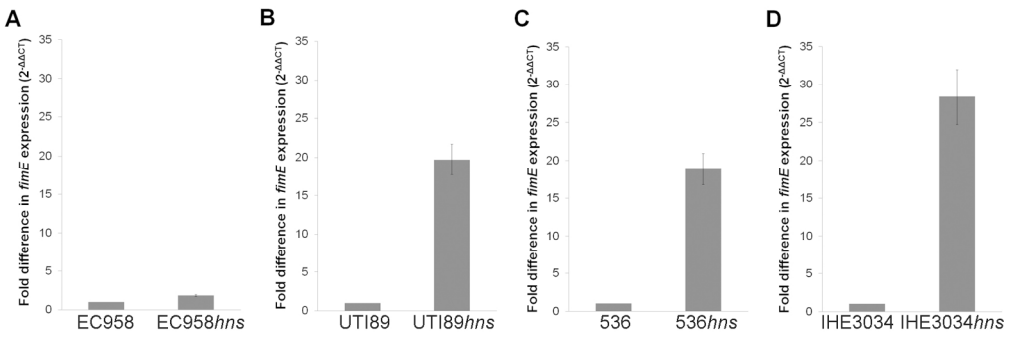

Fig. 7. Effect of hns deletion on fimE transcript level in different UPEC strains.
A. Fold-change in fimE transcription in EC958hns compared to wild-type EC958 as determined by qRT-PCR. B-D. Fold-change in fimE transcription in non-ST131 wild-type UPEC strains and their corresponding hns deletion mutants, namely UTI89 (B), 536 (C) and IHE3034 (D) as determined by qRT-PCR. Vertical bars represent means±SD of three independent replicates.
168x55mm (300 x 300 DPI)

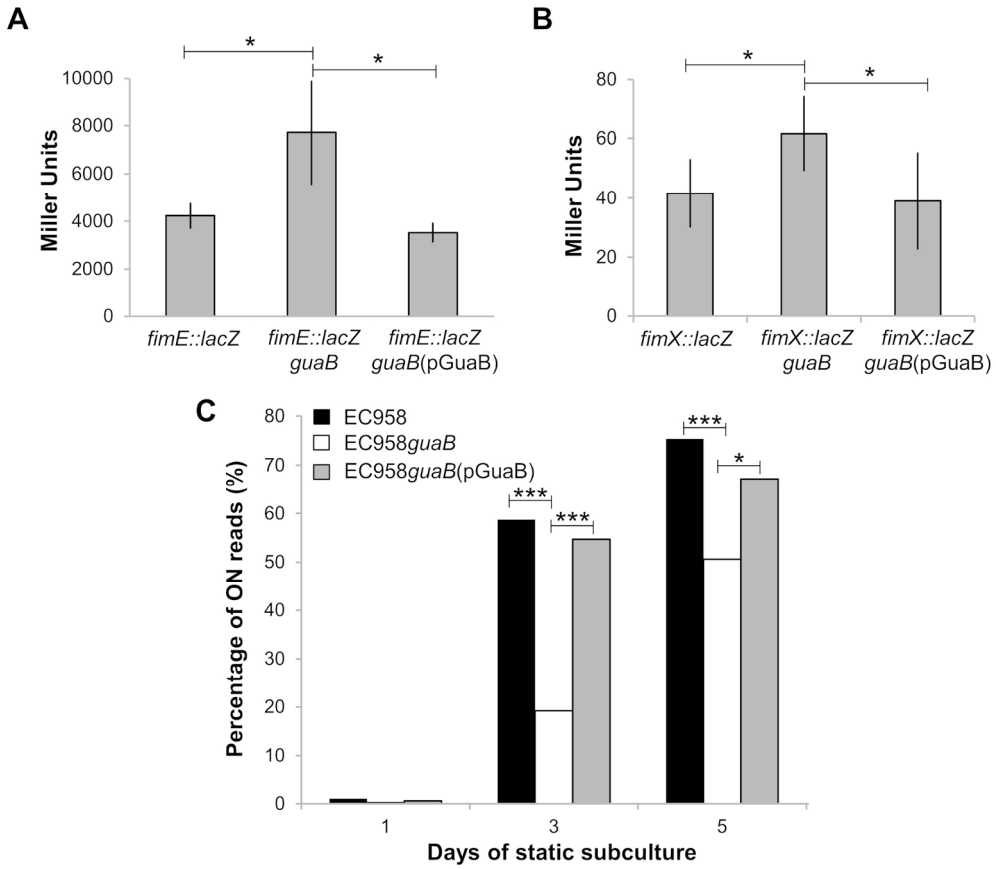

Fig. 8. Effect of guaB deletion on fimE/fimX promoter activity and fimS switching in EC958.
A-B. β-galactosidase activity of EC958 fimE (A) and fimX (B) promoter-lacZ reporter strains following overnight aerated growth in pooled human urine. All guaB mutant strains and complemented derivatives were constructed in their respective promoter-lacZ reporter backgrounds. Bars represent means ± SD of at least three independent biological experiments. Asterisk indicates a statistically significant difference ($P<0.05$) as determined by repeated-measures one-way ANOVA with Dunnett's multiple comparisons test.
C. DISCus analysis of the effect of guaB deletion on fimS switching. EC958 (wild-type), EC958guaB and EC958guaB(pGuaB) were grown statically in LB (37oC) over a period of 5 days. Over-expression of GuaB in EC958guaB(pGuaB) was induced by the addition of 1mM IPTG. Genomic DNA was extracted after static subculture on days 1, 3 and 5, and Illumina sequencing data was analyzed by DISCus. Bars represent percentage 'on' reads of fimS in each culture population. Asterisks indicate a statistically significant difference (* $P = 0.01$-0.001; *** $P < 0.0001$) as determined by a Pearson's $\chi 2$ test with Yates' continuity correction.
167x146mm (300 x 300 DPI)

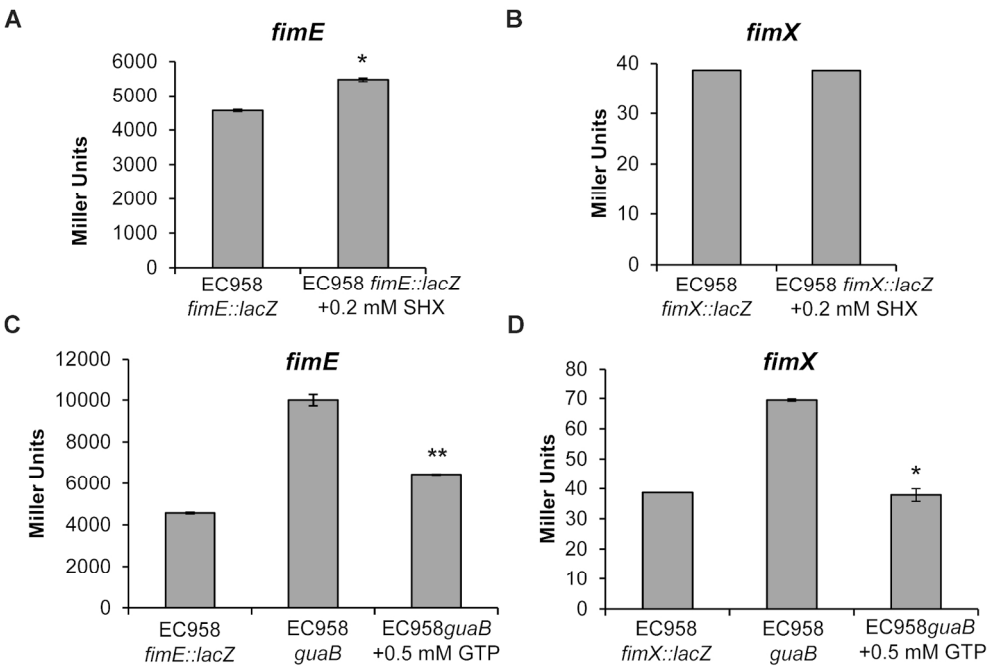

Fig. 9. Regulation of fimE and fimX promoter activity by (p)ppGpp.
A-B. Effect of serine hydroxamate (SHX, 0.2 mM) induced amino acid starvation on the promoter activity of fimE (A) and fimX (B) in EC958fimE:lacZ and EC958fimX:lacZ strains, respectively. All guaB mutant strains and complemented derivatives were constructed in their respective promoter-lacZ reporter backgrounds. Strains were incubated overnight under static conditions in pooled human urine and promoter activity was determined by the β-galactosidase assay. Bars represent means ± SD of three independent biological experiments with four technical replicates. Asterisk indicates a statistically significant difference ($P<0.05$) as determined by the Wilcoxon matched pairs signed-rank test.
C-D. Effect of GTP (0.5 mM) on the promoter activity of fimE (C) and fimX (D) in EC958fimE::lacZ guaB and EC958fimX::lacZ guaB strains, respectively. Asterisks indicate statistically significant differences (**$P<0.01$, *$P<0.05$) in guaB reporter strains upon addition of GTP, as determined by a repeated-measures one-way ANOVA with Dunnett's multiple comparisons test.
167x111mm (300 x 300 DPI)

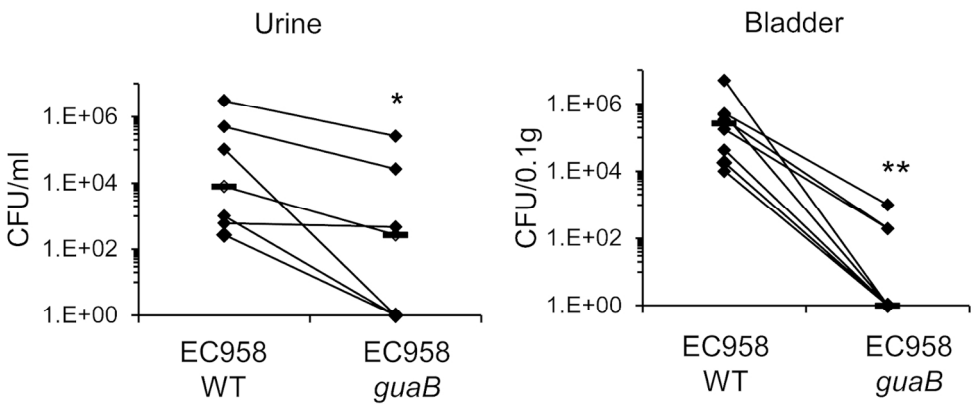

Fig. 10. Mouse urinary tract colonization by EC958 WT and EC958guaB. Female C57B/L6 mice were transurethrally inoculated with a 1:1 mixture of type 1 fimbriae enriched EC958 WT and EC958guaB strains in a competitive infection assay. Each marker represents total colony forming units (CFU) recovered from each mouse per 1 ml of urine or per 0.1 g of bladder tissue (as labelled) on selective medium. Lines connect data points for the same mouse and horizontal bars represent median values. Asterisk indicates statistically significant difference between the strains for persistence in urine ($P<0.05$) as well as bladder colonization ($P<0.01$) as determined by the Wilcoxon matched pairs signed-rank test.
150x61mm (300 x 300 DPI)